



SPE 113978-PP

Integrated Clustering/Geostatistical/Evolutionary Strategies Approach for 3D Reservoir Characterization and Assisted History-Matching in a Complex Carbonate Reservoir, SACROC Unit, Permian Basin

R. Gonzalez, SPE, K. Schepers, SPE, and S.R. Reeves, SPE, Advanced Resources International, Inc.; E. Eslinger, Eric Geoscience, Inc. and The College of Saint Rose; and T. Back, NuTech Solutions.

Copyright 2008, Society of Petroleum Engineers

This paper was prepared for presentation at the 2008 SPE Improved Oil Recovery Symposium held in Tulsa, Oklahoma, U.S.A., 19–23 April 2008.

This paper was selected for presentation by an SPE program committee following review of information contained in an abstract submitted by the author(s). Contents of the paper have not been reviewed by the Society of Petroleum Engineers and are subject to correction by the author(s). The material does not necessarily reflect any position of the Society of Petroleum Engineers, its officers, or members. Electronic reproduction, distribution, or storage of any part of this paper without the written consent of the Society of Petroleum Engineers is prohibited. Permission to reproduce in print is restricted to an abstract of not more than 300 words; illustrations may not be copied. The abstract must contain conspicuous acknowledgment of SPE copyright.

Abstract

An integrated methodology combining clustering analysis techniques, geostatistical methods and evolutionary strategy technologies was developed and applied to an area in the SACROC Unit (Permian basin). Clustering methods were applied to well logs and core data with high vertical resolution for many wells to predict porosity, permeability and rock type. Geostatistics was applied to extend the characterization into the inter-well area. Evolutionary strategies were used to refine the characterization to match historical production performance.

The complete approach was tested on an area within the SACROC Unit, acknowledged as a highly heterogeneous carbonate reservoir with complex production history. Three cored wells provided porosity and permeability measurements on a foot-by-foot basis. These measurements coupled with well logs were used to predict porosity, permeability and flow units. Twenty two wells in the study area having foot-by-foot profiles of porosity and permeability were considered sufficient to characterize porosity and permeability in three dimensions. Geostatistical methods were then used to build porosity and permeability models.

As a validation of the characterization procedure, evolutionary strategy jointly coupled with a black oil reservoir model was used to history match production performance of a 0.5 mi² area. The 65,340 grid-block model had over 50 years of production. Thirteen (13) input parameters were varied during the history match. Among them, a multiplying factor was applied to the permeability realization to account for upscaling effects, varying permeability values without modifying geological heterogeneities identified during the characterization process. No adjustment to porosity characterization was permitted.

A very good history match of individual production was achieved for the center wells of the area, and a good match was also obtained for outer wells production and reservoir pressure where boundary effects existed. This validates the new integrated clustering/geostatistical/evolutionary-strategy approach in this highly heterogeneous carbonate reservoir.

Introduction

An integrated methodology combining clustering analysis techniques, geostatistical methods and evolutionary strategy technologies was developed and applied to a study area in the SACROC Unit (Permian basin). Initially, a two-step “soft-computing” procedure was developed capable of efficiently generating core-scale porosity and permeability profiles at well locations where no core data existed. The approach applies clustering methods based on maximum likelihood principles to well logs and core data for lithology interpretation, reservoir quality characterization, and prediction of “core” parameter profiles, with high vertical resolution for many wells. This procedure permits to populate any well location with core-scale estimates of porosity and permeability (P&P), and rock types facilitating direct application of geostatistical techniques to build 3D reservoir models. Geostatistical methods are then applied to the resulting dataset, and three-dimensional spatial models of variability for clusters, porosity, and permeability are utilized to generate reservoir representations of P&P for flow simulation purposes. Finally, a computer assisted history matching based on application of evolutionary strategy technologies

was used to history match the production performance of a selected subregion in the SACROC Unit (Permian basin).

The complete approach was applied in a selected area within the SACROC Unit platform, acknowledged as a highly complex carbonate reservoir and with complex production history. The studied rocks belong to the Pennsylvanian-aged Cisco and Canyon Formations in the SACROC Unit which covers the majority of the Kelly-Snyder field. Three wells were drilled in the platform, fully cored through the reservoir (~ 800 ft) and porosity and permeability measurements taken on a foot-by-foot basis (one of these wells is in the study area). These measurements jointly with modern well logs were utilized to develop models that firstly predict acoustic impedance, product of bulk density (RHOB) and delta time (DT), from only gamma-ray (GR) and neutron porosity (NPHI) logs (widely available), and secondly P&P from these three combined logs.

Data from twenty-two wells in the study area and two external cored wells were selected for clustering analysis. Firstly, rock types of similar depositional environment and/or reservoir quality were discriminated using a model-based, probabilistic clustering analysis procedure called GAML^{1,2,3,4} (Geologic Analysis via Maximum Likelihood System). During clustering, samples (data at each digitized depth from each well) are probabilistically assigned to a previously specified number of clusters with a fractional probability that varies between zero and one. This permits individual samples to have characteristics of more than one "rock type" or reservoir quality unit, and so allows for gradational, or intermediate, rock types. The "taxonomy" developed from this classification procedure is used as a framework for ensuing calculation of reservoir parameter values. Details of the clustering analysis work flow are given in reference 3.

The modes were qualitatively related to reservoir quality using data output tables, crossplots, and frequency plots. Also, cross sections were generated which permitted a visual and qualitative assessment of lateral "bed" continuity and vertical bed thickness and style. Synthetic well logs were generated for wells with incomplete log suites and also estimated values of P&P for wells with no core data. This information was used to help define flow units and reservoir properties. The existence of twenty two (22) wells in the study area having foot-by-foot profiles of P&P was considered sufficient information to characterize directly the reservoir distributions of porosity and permeability. In consequence, stochastic simulation algorithms were utilized to provide reservoir characterizations of P&P in the selected study region with different levels of vertical resolution.

As a measure of validation of the previous characterization procedure, a computer assisted history matching of prior production was achieved without significant changes to the original characterization of the studied region, and utilizing evolutionary strategy methodology. In recent years, computer assisted history matching has acquired a relevant role in the practice of reservoir simulation, as a consequence of increasing computer power, more complex reservoir models, and shortage of experienced personnel. In particular, evolutionary strategy technology has been favored over other techniques commonly used (gradient based methods, genetic algorithms, etc) when complex optimization problems with many variables and target functions are faced (typical of reservoir simulation history matching).

In this work, evolutionary strategy technology was applied in a black oil reservoir simulation model to history match the production performance of a ½ mi² area containing 22 wells in the SACROC Unit. Production from the field is primarily from the Upper Pennsylvanian Canyon Reef reservoir, which can be as thick as 900 feet in the study area. The 65,340 grid-blocks model had over 50 years of production, injection and reservoir pressure history to match. A total of 13 input parameters were unavailable for the study and varied during the assisted history matching to reaching optimized values. Among parameters to be optimized, a permeability multiplying factor was included to be directly applied to permeability values populating the model grid-blocks without varying geological trends and heterogeneities that were identified during the characterization process.

Due to the importance of the influxes in the modeled region, several techniques to estimate water influxes were applied in order to define proper boundary conditions. Using the evolutionary strategy technology, a very good history match was achieved of individual oil production, water production, and gas production history for the center wells of the study area, and a good match was also obtained for the outer producing wells. History matching of the outer wells production was well achieved thanks to the optimized boundary effect. A good reservoir pressure match was also achieved, even though some necessary simplifications. Hence, this simple black oil model was accurate enough to understand the reservoir behavior of SACROC Unit, Canyon Reef Formation. This seems to validate the applicability of the new integrated Clustering/Geostatistical/ Evolutionary-Strategies approach in this highly heterogeneous carbonate reservoir.

Area of Study

The SACROC Unit comprises most of the Kelly-Snyder field and some of the Diamond "M" field in Scurry County, Texas. It is a part of the Horseshoe Atoll located in the eastern half of the Midland Basin which is the eastern sub-basin of the overall Permian Basin of western Texas and southeastern New Mexico (Figure 1). The SACROC is developed in

Pennsylvanian aged reef carbonates of the Cisco and Canyon formations with productive carbonates actually belonging to both formations^{5,6}. The productive interval is composed mainly of limestone, although minor amounts of anhydrite, chert, sandstone, and shale can be found locally. Dolostone is rare to nonexistent. The overlying Wolfcamp shale constitutes a natural top and lateral seal. Towards its East and West boundaries, the Cisco-Canyon productive carbonate interval narrows and drops below the regional oil-water contact. Carbonate accumulations present extremely complex geometries and steep sides, and seem to frequently commence on antecedent highs in one or more underlying zones. Sea level fluctuations during Pennsylvanian time were likely the dominant controls on the various facies developed across the reef and on the productivity of the "carbonate factory"^{5,6}.

These depositional complexities, accompanied by some probable intermittent subaerial exposure with associated dissolution and karsting, resulted in a complex reservoir stratigraphy where flow unit lateral continuity beyond a few hundred feet is perhaps the exception. For instance, Raines et al^{5,7} presented how two wells spaced only 250 ft apart exhibit substantial differences in the vertical distribution of porosity. Additionally, later production operations and treatment techniques have also impacted reservoir response, primarily through reservoir fracturing and localized pressure modifications. Thus, the complicated nature of this reservoir can be attributed to a variety of natural and man-made processes.

Well Log Data

Data from more than four hundred (400) wells from the platform were available for study. These wells are of a variety of ages and many do not have a "full" well log suite.

The most relevant log parameters for the characterization tasks were determined by applying multivariable statistical methods⁸, and taken into consideration other aspects like capabilities of each log tool, and log availability in each well. The well log parameters judged best suitable for characterization tasks were RHOB, NPHI, GR, and DT. Wells with these four logs were considered as having a "full" log suite. Unfortunately in the SACROC unit, the absence of RHOB and/or DT logs is the most common well condition. In the subregion used for this study, only four (4) wells had a full log suite; however, for clustering purposes, other six wells near to the study area and the two external cored wells were utilized.

As discussed in more detail in references 8 and 11, to reduce the number of total variables in the clustering runs and in some specific stages of the whole characterization process, existing RHOB and DT logs were utilized to generate an acoustic impedance well log (herefore denoted as AI_log) as a combined form of both logs. AI_log was computed as $AI_log = 100 (RHOB/DT)$.

Core Data

The three cored wells (cored between 2004 and 2005) were wells 11-15, 19-12, and 37-11, and only the well 37-11 was near the center of the study area (Figure 2). Porosity and permeability data at one-foot intervals were available from these wells over the entire interval (~ 800 ft). There were 26 older wells with some core data, but measurements type and quality of the porosity and permeability analyses from these wells were not believed to be comparable with the new core data.

In general terms, core data indicates that porosity tends to increase down-section in the upper half of this interval and then decreases through the lower part of this interval. The core permeability (more specifically its logarithm value) follows a similar trend. Due to the thin-bedded nature of flow units, these changes are not smooth with depth, and the well logs often do not have sufficient resolution to detect the rapid vertical changes in permeability.

The porosity and permeability data used here are measurements taken from whole core at one foot sampling intervals. Three values for permeability were measured on every sample: K0, K90, and KV. K0 and K90 whole core measurements (WCM) were measured relative to a master orientation line in order to identify any directional bias in the horizontal permeability⁹. Both horizontal permeabilities have similar ranges, and they have a similar density profile. Indeed, a direct comparison of logarithm of K0 and logarithm of K90 via cross-plots shows that the values are well aligned around the coincidence line of unity slope. Figure 3 show all cored wells discriminated by colors.

The absence of significant variation in the logarithm of permeability suggests that there is not a strong horizontal directional bias at these locations. Consequently, we considered K0 to be representative of the horizontal permeability, and concentrate our analyses on this parameter based on the fact that no noticeable directional bias of this permeability data was identified. This conclusion was assumed for the whole North Platform because all three cores drilled have sampled all or almost all of the Cisco Formation.

The relationship between WCM of permeability (K0) and WCM of porosity for the three cored wells is shown in Figure 4.

Despite linear-like "cloud" trends there is not a strong linear relationship between the logarithm of permeability (K0) and porosity for any of the wells. This is not unexpected because the reservoir is made of different depositional facies each of which might be expected to have different porosity-permeability relationships.

Two different central measures for porosity and logarithm of permeability (K0) were calculated for all samples to investigate the levels of correlation between $\log_{10}(K0)$ and porosity. These central measures were an arithmetic mean value and a median value corresponding to an adopted size-window around the sample depth⁸. From inspecting those average values, it was concluded that P&P experience a slight increase in correlation as the window sizes are incremented. Further details and discussion can be seen in reference 8.

Discrimination and Interpretation of Facies Units

Lithologies were discriminated and interpreted using the probabilistic clustering analysis procedure^{3,4}. This soft-computing procedure permits well logs, seismic attributes and core reservoir parameters to be used as variables in a multi-dimensional clustering analysis that results in all samples (at their respective depths) being assigned probabilistically to a user-defined number of "modes". A "mode" is a mathematical term that has the same functional meaning as "cluster." The modes can be envisioned as electrofacies (or lithofacies or flow units) having similar properties^{3,4}.

Since the sample assignments at each depth are probabilistic, each sample can be assigned probabilistically to more than one mode or facies unit. This is referred to as the "fuzzy" probability assignment, and is in concurrence with the idea that although ideal end-member rock types might exist (e.g., "clean" sandstone, "pure" limestone ...), many rocks might have a composition intermediate between two or more end-member rock types. In a depth plot, the "fuzzy" probabilistic assignments are displayed as a stacked bar chart on a horizontal axis with axis ranging from zero (probability) at left to 1.0 (probability) at right. The sum of the mode probability assignments at each depth or sample is 1.0 (see Figure 7). Lithology assignments for each of the clustering modes (facies units) can be tentatively assigned. This is based largely on GR signal for clastic rocks and apparent grain density for carbonate rocks¹⁰. Depth plots that display the probability assignments of all samples can be used to provide an easy method for visual examination and interpretation.

The term "facies" is used above as the name for a group of samples that have similar well log character as defined by a cluster analysis. However, we use the term "mode", "facies", "rock type", and "flow unit" interchangeably. This last term, understanding that one or more of the included variables is a flow property (such as permeability) or is related to a flow property (which most well log curves are).

Reservoir Quality of Facies and Flow Units

A major goal of this study is to define flow units and to determine their Reservoir Quality (RQ). We here use RQ to mean the porosity, permeability, bed thickness, and lateral bed continuity of the flow units. But, only porosity and permeability are evaluated in a quantitative manner. Flow units can be defined by clustering analyses using well log curves as variables or a combination of well log curves and core permeability and core porosity. There are several different work flows that can result in determination of the RQ of flow unit realizations. It is not obvious, a priori, which work flow will produce the most realistic flow unit realization and which work flow will produce the most credible definition of RQ for any given flow unit realization. However, it was shown^{8,11} that the modeling procedure is quite robust in that the porosity and permeability profiles obtained are largely independent of the particular work flow used.

Since only three reliable cored wells were available, and only one of them is in the study area, the database for building a model for estimating porosity and permeability for the non-cored wells was limited in terms of areal extent across the studied area. However, because the cored wells were sampled every foot over a depth range of about 600 to 900 feet each, a considerable amount of core data was available for use

For each clustering run, or series of clustering runs, the realization provides the following information for each flow unit:

- the arithmetic mean and standard deviation of porosity,
- the arithmetic mean and standard deviation of the logarithm (base 10) of permeability,
- the total bed thickness, the number of beds, and the average bed thickness for the original beds (defined by clustering),
- qualitative assessment of well-to-well lateral continuity of each flow unit. This is done by generating for each well either a depth plot of the "fuzzy" probabilistic assignment or a depth plot of the "crisp" (mode) assignment and correlating these among wells by visual examination.

Estimation of Porosity and Permeability in Non-Cored Wells

The basic approach is to perform a clustering run using one or more cored wells with core porosity and/or core permeability as variables along with a selected log curve suite as variables. For any non-cored wells included in the clustering run, estimates of core porosity and/or core permeability can be automatically made during the clustering process.

Since most of the wells had no RHOB or DT logs, the decision as to whether to "fill in" the "ideal" log suite by estimating both RHOB and DT profiles for these wells (using the clustering methods), or to combine these two variables into only one variable, acoustic impedance (AI_log), also needed to be made. Both approaches were tested, but the latter method (calculation of log AI_log) provided the opportunity of having a log-based parameter that could possibly be correlated with the seismic acoustic impedance and that could also be used in clustering runs that included both well log and seismic attributes. Besides, the use of AI_log instead of RHOB and DT decreases by one the number of variables when clustering processes are later carried out using wells having only GR and NPHI.

Clustering runs were done both ways to verify the effectiveness of using AI_log instead of RHOB and DT in order to predict porosity and permeability values. Predicted porosity and permeability values generated using the clustering run that utilized GR, NPHI and AI_log, were not significantly different from the predicted values generated using the clustering run that utilized GR, NPHI, RHOB and DT. Both clustering runs also included as variables the core porosity and core permeability (\log_{10}) from wells 37-11 and 19-12 (cored well 11-15 was preserved as a "hold out" well and so was not included in the clustering runs.). The results are shown in references 8 and 11.

The procedure for combining RHOB and DT into AI_log and then using AI_log as a clustering variable is herein termed the "P&P via AI" method. This method involves several clustering runs which included AI_log, selected additional log curves (NPHI and GR), plus one or both permeability and porosity. The end results are "predicted" profiles for porosity and permeability in non-cored wells. The "P&P via AI" method is described in a step-wise manner in references 8 and 11.

Figure 5 shows tracks of AI_log, core porosity, and core $\log_{10}(K0)$ respectively for cored well 11-15, the hold-out well. Actual values are in red and predicted values are in blue. These results were obtained during the sequence of different clustering runs done during establishing the "P&P via AI" method. For instance, cluster C1 was the first clustering run used to predict AI_log at wells. This cluster C1 had identical conditions to cluster C2 except that well 11-15 was excluded. The first two tracks indicate that agreement between predicted values and actual values are pretty good. In the track for $\log_{10}(K0)$, we can appreciate that spatial tendencies are reproduced; however, larger numerical differences between actual and predicted values are evident. Figure 6 shows cross plots of predicted vs. actual values. AI_log is shown at left; porosity is seen at center, and $\log_{10}(K0)$ is exposed at left. All cross plots show a good alignment reflecting a definitive correlation between predicted and actual values. The corresponding correlation coefficients (r) are 0.94 for AI_log, 0.74 for porosity, and 0.59 for $\log_{10}(K0)$. As it can be expected for permeability, its prediction is the least accurate in absolute terms. However, the vertical variability of permeability is reproduced quite well; the predictions simply do not fully capture the extreme values. Nevertheless, reproducing the vertical variability is arguably the most important objective when utilizing such results for reservoir flow simulation purposes. More details about this subject are given in Appendix A of reference 11.

Clustering results and raw logs are shown for two of the cored wells in Figure 7. For each well, the first track shows GR and DT and the second track show RHOB and NPHI. The third and fourth tracks are core porosity and core permeability, respectively. The fifth track is a Cumulative Mode Probability (CMP) plot which displays the "fuzzy" probabilistic assignment at each depth (the horizontal axis is fractional probability). The sixth track is a "beds" plot which displays the "crisp" (mode) assignment at each depth (only the mode is shown that has the highest probability for each sample depth). The CMP plot is also termed a "fuzzy" plot and the "beds" plot is also termed a "crisp" plot.

We used a combination of the "ModeAssign" routine (which gives default lithologies for each mode), some user decisions, and previously reported information about the SACROC to interpret all of the modes that comprise the Cisco and Canyon interval to be limestones. Independent of the core data, Mode 10 (M10) was interpreted to have the best RQ because it had the highest mean NPHI value (0.13) which in turn suggested that it had the highest porosity in these fairly "pure" calcite-rich rocks. That is, in these clay-poor rocks, NPHI appears to be a fair indicator of porosity.

The relative ranking of RQ based on mean NPHI values was confirmed by the core data. A table generated as part of the clustering results that gives mean core porosity and permeability for each mode showed^{8,11} that M10 generally had the best RQ in the cored wells. This mode, the apparent "best" limestone, was named (M10_LsBest). For plotting purposes, this mode was assigned a bright red color. M10 plus six other modes, also interpreted to be limestones, comprise nearly all the Cisco and Canyon interval.

Of the other six limestone modes, three had relatively high apparent porosities based on the mean NPHI values: M3_LS1

with mean NPHI = 0.12, and M5_LS2 and M8_LS3 with mean NPHI = 0.11. The other three limestone modes had relatively low apparent porosities: M1, M7, and M2 with mean NPHI values of 0.04, 0.04, and 0.01, respectively. To discriminate among the "high porosity" modes and the "low porosity" modes, M3, M5, and M8 were colored deep pink, hot pink, and pink, respectively, and the other limestone modes were shades of blue (the deeper the blue shade, the lower the porosity). The modes assigned as siltstones (M9_Slt, green) and shales (M6_Sh1, M4_Sh2, grays) were mostly (but not entirely) above the carbonate sections and presumably mostly in the overlying Wolfcamp shales. The upsection change from carbonates to shales indicated by the clustering results is generally sharp and provides a good way to pick the contact between the Cisco and the Wolfcamp.

In summary, the "P&P via AI" method allowed populating all wells included in the selected subregion with core-scale P&P curves which facilitated the application of geostatistical methods for reservoir characterization of the subregion.

The Geostatistical Approach

The existence of twenty two (22) wells in the study area having foot-by-foot profiles of P&P was considered sufficient information to characterize directly the reservoir distributions of porosity and permeability. Stochastic simulation algorithms were utilized to provide reservoir models of porosity and permeability in the selected study region with different levels of vertical resolution. The goal was to generate reservoir parameter characterizations with an appropriate vertical resolution to aid the efficient characterization of this complex reservoir.

In general terms, hybrid simulation approaches that combine two or more conditional simulation techniques are used in a geostatistical study^{12,13,14}. A geostatistical reservoir characterization based on a hybrid approach usually consists firstly in building the reservoir architecture where the geometry of the units is established; then, determining the geological model where geobodies are populated with lithofacies, and finally generating the petrophysical model where distributions of typical reservoir parameters are assigned to each facies.

Object-based methods are suitable to describe reservoirs with certain geometric features, provided that adequate information (qualitative and/or quantitative) of the geometry of reservoir bodies is available^{12,15}. However, object-based modeling is less applicable to carbonate environments which have facies that exhibit serious post-depositional processes (dissolution, re-precipitation, dolomitization, fracturing, etc) that have deteriorated the geometry of their shape such that the utilization of known geometric objects and the estimation of their dimensions are problematic. Due to the above argument, and given the existence of twenty two (22) wells in the study area with profiles of P&P, variogram analysis was directly applied to this data to determine possible patterns of spatial variability of these parameters. With the derived variogram models, the Sequential Gaussian Simulation (SGS) algorithm conditioned to the well data was used to generate multiple reservoir distributions of porosity and permeability at interwell locations. Corresponding central scenarios of P&P were generated from these characterizations and were utilized as input into the next step, reservoir simulation performance, where production data have to be honored.

Variogram Analysis

For the variogram analysis of SACROC, actual values and pseudo values of core porosity, core permeability, and rock types were utilized to calculate corresponding experimental variograms. In order to calculate the experimental variograms of P&P and modes (rock types), a stratigraphic or conformal transformation of vertical coordinates was first carried out in order to compare samples from similar stratigraphic horizons and to avoid typical differences resulting from horizontal slicing based on the original coordinate system^{8,11}. This kind of "unrolling" of the structure allows comparison of sample values at the same "stratigraphic horizon" when the experimental variogram is calculated. Comparisons of samples under this premise are considered geologically consistent because it can be expected that reservoir parameter values at the same "stratigraphic horizon" have more depositional similarities. In consequence, resulting experimental variograms can better reveal the "hidden" spatial behavior of the variable under analysis.

Due to the dimensions of the subregion under study, to the significant number of wells included in it having foot-by-foot profiles of porosity and permeability, and to practical considerations related with the posterior task of the flow simulation (data availability, simulation objectives, grid definition, software, etc.), it was decided to characterize directly the distribution of P&P without the consideration of the rock type parameter (mode) as a possible guide. In addition, the origin of the foot-by-foot P&P pseudo values at well locations is narrowly tied to the corresponding foot-by-foot mode or rock type values at the same well locations, so this fact also favors the direct and less elaborate approach. However, some indicator variogram analyses of modes (rock types) and variography studies of P&P for each rock type were carried out in order to complement the global variography of P&P.

The use of Gaussian techniques requires a prior Gaussian transform of the data and the complete variogram analysis of these transformed data (experimental and modeling tasks). The public domain software SGEMS (Stanford Geostatistical Earth Modeling Software)¹⁶ which was used to compute the experimental variograms of normalized porosity values, normalized permeability measurements (log10), and rock-types in both the vertical and horizontal directions, and fit spherical variogram models to the experimental variograms, as long as there was adequate data to estimate the experimental variogram in the considered direction and for the considered variable. In summary, the parameters describing the spatial correlation (nugget effect, sill, number of structures, types of structures, and ranges) were obtained graphically by plotting the experimental variogram against intersample distances and then fitting corresponding theoretical models.

The nugget effect value and general structure of the models were obtained from vertical variograms, and were extended to horizontal (areal) variograms. Directional variograms were constructed in eight directions under the assumption that the stratigraphic transformation of coordinates produces the effect of sample pairs belong to the same bedding plane or stratigraphic horizon.

In the reef-carbonate depositional environment of SACROC, different scales of variability can be seen, for instance, in variograms of porosity, and these different scales of variability were modeled using nested variograms (linear combinations). Porosity values at well locations (actual measurements and pseudo data) were initially normally transformed prior to the variography study. The vertical variogram analysis of porosity indicated a behavior described as a combination of spherical (or exponential) and dampened hole-effect (cyclic) variograms^{12,17}. In SACROC, this cyclicity effect in the vertical direction can be associated with the carbonate buildups. Relative sea level “rise and fall” occurred repeatedly, providing a variety of depositional environments and facies that repeat with geological time (seen in depth).

Horizontal experimental variograms were calculated^{8,11} in the directions 0°, 30°, 45°, 60°, 90°, 120°, 135°, and 150° (angles are measured clockwise from the axis North-South 0°). The dampened hole-effect structure is not seen in these directional experimental variograms of normalized porosity. For this reason, the experimental variogram in the vertical direction was modeled as a combination of a nugget effect component and two nested structures conceived as spherical models of spatial variability. A model of geometric anisotropy was adopted for describing the horizontal spatial variability of (normalized) P&P for this SACROC study area. The horizontal model was constructed using an isotropic nugget structure and two structures with geometric anisotropy reflecting an intermediate and a global scale. Variance values (sill, relative sill, and nugget effect) of horizontal models honor those values derived from the vertical variography. The major scale reflects a spatial variability aligned in the direction of the main structural trend of the reservoir. This greater variogram range along the direction of the structural axis can be explained by the constructional characteristics of the SACROC limestone reef. The intermediate scale of variability tends to be more isotropic, and can be associated with complex patterns of sediment deposition that provided later opportunities for erosion and diagenesis.

Some facts for the building of the permeability variogram model were “borrowed” from the variogram modeling of porosity¹⁸. This was supported by the different correlations established from core data^{8,11} and the cross variogram analysis. With the purpose of complementing the modeling of spatial continuity of P&P, indicator variograms were also developed for rock type (modes) values derived from the clustering analysis methodology applied in this work^{11,19}.

Geostatistical Models

In order to validate possible representations of P&P for this area, a reservoir flow simulation exercise was designed. In essence, the goal is to match the history of some relevant production parameters in this part of the reservoir. Due to the related nature between the characterization task and the flow simulation activity, some decisions about the geostatistical characterization plan were made. In addition to the arguments already exhibited for a direct characterization of P&P, the lack of more detailed information of reservoir-rock and fluid properties had impact on the decision of using a black-oil simulator instead of a compositional one. This in turn resulted in a more confident acceptance of the reservoir distribution of P&P directly obtained from those values (actual and pseudo) at well locations. More details about the data availability and other flow simulation aspects²⁰ are exposed later. We use a commercial simulation software²¹ which is a black oil simulator that models the flow of three phase flow in gas, gas-water, oil-water, and oil-water-gas in 3D reservoirs.

The study area was selected jointly with the operator Kinder Morgan CO2 Company, L.P (KMCO2) based on the existence of a completely cored well in this area (well 37-11), a planned cross-well seismic survey inside the area, and a possible CO2 injection procedure to be implemented in there. The study area is 0.7 mi by 0.7 mi by 780 ft of average thickness (area of 313.6 acre). There are 22 wells in the study area, but only 1 cored well with actual P&P data. The remaining wells have pseudo values of these reservoir parameters derived through the soft-computing methodology adopted for this work. All wells were considered vertical for practical purposes. The producing region has been active for almost 60 years, and over 50

years of well performance history is available to simulate the study area.

For the P&P geostatistical characterizations, it was decided to propose a grid definition that could work directly in the flow simulator. Both the geostatistical characterizations and the reservoir flow simulations were conducted on the same Cartesian grid. The study area was discretized in both grids with 33 cells in the East-West (X) direction, 33 cells in the North-South (Y) direction, and with 60 layers (Z). The grid block dimensions were respectively 112 ft, 112 ft, and 15 ft.

SGS characterization

The geostatistical simulation task in this work had as an objective the generation of a legitimate representation of the spatial distribution of porosity and permeability in the study area as a part of the combined procedure of characterization (clustering/geostatistic) implemented in this project. Calculations were carried out on the same reservoir volume used for the fluid flow simulation study and with the same grid definition. For both porosity and permeability, the SGS technique was applied to interpolate data and to obtain multiple equiprobable realizations.

Sequential Gaussian Simulation is the most popular and straightforward algorithm to generate possible spatial representations of a reservoir parameter. Simulation is executed sequentially using the conditional cumulative distribution function derived by solving a kriging system^{12,13,14,22}. The simulation technique produces several possible realizations, and each realization generally reproduces the characteristics of the input variable. Each simulated realization can be forced, or not forced, to honor the constraining well data depending on the particular case study. SGS procedure relies on the multi-gaussian framework and, generally, requires a prior transformation of the information (from the raw set of samples to the Gaussian space) as well as a posterior back transformation of the Gaussian simulated results to the original scale of data.

Porosity Model

Using the derived variogram model of porosity, and the SGEMS program *sgsim*, twenty (20) realizations were generated describing possible distributions of this parameter. An “average” image of all 20 realizations is shown in Figure 8 jointly with an image of wells positioned inside the subregion. This “box” displays the spatial distribution of porosity in a perfect rectangular domain that represents, after the stratigraphic coordinate transformation, the selected area under study. This and all related images about the characterization procedure were produced by the software SGEMS. These 3D images have the peculiarity of describing increasing vertical values from bottom upwards, so the deepest reservoir layer is seen on the top of the reservoir-box while the shallowest layer of the reservoir is the reservoir-box bottom. In this study, the “average” image drawn from the 20 equiprobable realizations is derived, at each grid block, by the arithmetic mean of the different simulated values assigned to such grid block in each different realization. This central scenario was adopted as the final model for flow simulation purposes. Some wells were addressed for reference purposes with their corresponding porosity values. The model is read in terms of fractions.

Permeability Model

Based on the assumed correlation between porosity and logarithm of permeability, the SGS algorithm was adopted again to simulate the logarithm of permeability now supplemented by the model adopted for porosity in this region as parameter guide. For cosimulation tasks, SGEMS provides the program *cosgsim* which allows simulating a Gaussian variable accounting for secondary information. The cosimulation approach adopted here was to utilize the dependence of the secondary variable on the primary, limited only to the co-located primary variable, with the cross-variogram proportional to the variogram of the primary variable. This option also requires a correlation coefficient value between the variable to be simulated (primary) and the variable used as guide (secondary). Based on the window averaged analysis developed between the logarithm of permeability and porosity (see references 8 and 11), a value of 0.725 was adopted when the 20 different realizations of logarithm of permeability were generated.

Figure 9 shows the averaged model of logarithm of permeability (left) jointly with the final model of permeability (right). As the final model of permeability, each value $\log_{10}(K_0)$ was back-transformed by using the exponential function (base 10) given by $f(x) = 10^x$. This permeability model is read in terms of millidarcies (md). Additional details about these two geostatistical models are given in references 11 and 19. As a final task, the box-shaped models of P&P were back transformed to the original coordinates. Geostatistical surfaces of top and bottom were used for the forward and back transformation of coordinates. Results¹⁹ are not here presented.

Reservoir Simulation Methodology

The reservoir model built in this study covers an area selected jointly with the operator KMCO₂. Porosity and permeability distributions were defined using geostatistical characterizations as described in previous sections, and with more detail in references 11 and 19. KMCO₂ provided production and injection data, and PVT and formation data came from published literature. A black oil model of more than 65,000 grid-blocks was build which included the 19 producing wells and 3 injecting wells.

The ability to reproduce proper boundary conditions at the edge of the model was critical to achieve a good match. Boundary conditions at the edge of the models were calculated using several different methods (simple large scale reservoir model, differential water volume calculations, and material balance). Pseudo wells were incorporated at the edge of the modeled area to reproduce water fluxes. However, some uncertainties remained because the different methods gave different answers. Therefore, a factor controlling water fluxes at the edge of the model was used, and was optimized during the history matching process.

For each individual producing well included in the study area, liquid, water and gas production rates were history matched. We were confident in the upscaling of porosity; hence, original porosity realization was used as-is in the reservoir model. However, it was anticipated that upscaled permeability would probably underestimate actual permeability. To preserve geological trends and heterogeneities, the original permeability characterization was used but was multiplied by a factor between 1 and 5 that needed to be optimized during the history matching process.

The final objective was to understand and to reproduce the reservoir performance of Canyon Reef formation in the Kelly-Snyder field using a simple but accurate black-oil model. The history matching would be achieved by using an automated optimization process.

Reservoir Model

The modeled sector represents the area covered by the geostatistical realizations for porosity and permeability here presented^{8,19}. A commercial reservoir simulator was used in this study²¹. The model consists of 65,340 grid-blocks (33 x 33 x 60), each grid block being 112 ft by 112 ft in the horizontal direction and 60 layers 15 ft thick each. All 19 producers and 3 Water Alternating Gas (WAG) injectors are included in the model. The 3 injectors were originally producers, converted to water injectors and finally converted to WAG, as indicated by actual production history. The completion history for each individual well was respected since this information had been provided by KMCO₂. The total area covered by the model is hence 13,660,416 ft² or 313.6 acres. The Original Oil In Place (OOIP) for this model was 89.4 MMSTB which only represents a small percentage of the 49,900 acres SACROC region, with OOIP estimated at 2,113 MMSTB²³.

Reservoir characterization

Porosity and permeability models defined by clustering analysis were used here. Average porosity of this heterogeneous model was 8.5%. Average permeability of this characterization was 2.74mD. Figure 10 presents the porosity characterization implemented inside the reservoir model (simulator graphic displaying). Figure 11 presents the horizontal permeability incorporated into the reservoir model. No permeability anisotropy was introduced (between K_x and K_y) because results derived from the integrated clustering/geostatistical approach for the characterization accounted for it^{8,11,19}. Table 1 summarizes the other reservoir properties used during the simulation.

Fluid Data

Few fluid data were available at the time this study started. The PVT data used in this study came from the published literature^{24,25,26,27} and commonly used PVT correlations. The available data and their sources are summarized in Tables 2, 3 and 4.

Oil-Brine Relative Permeability measurements were available from KMCO₂ and include four samples for wells 32-3 and 34-6. Those data are presented in Figures 12 and 13. No gas-water relative permeability curves were available for the study. Seven (7) measurements of centrifugal capillary pressure curves coming from well 65-4 were provided by KMCO₂. Two samples had the closest permeability value from the average permeability used in the model. Due to the coherence between those two samples, it was decided to keep a constant capillary curve inside the reservoir model; and an average curve of the two samples was used. It is presented in Figure 14. Centrifugal capillary pressure curves are known to accurately define irreducible water saturation. From these samples, irreducible water saturation varied from 0.22 to 0.38. No gas-oil capillary pressure curve was available from the operator or in the published literature. Since CO₂ displacement can not be modeled

accurately by using a black oil model, it was decided to ignore the gas-liquid capillary effect.

Only one rock type was defined in this model. From the relative permeability samples of wells 32-3 and 34-3, relative permeability (K_r) curves endpoints vary significantly, so it was decided to vary oil-water and gas-liquid relative permeability endpoints and shape using Corey's functions during the optimization process. An initial water-oil contact was present in SACROC field Canyon Reef reservoir at a depth of 4,500 ft subsea. This information can be found in the literature^{24,25,27,28,29} and is very coherent from one paper to another.

Production Data and Model Control

Production data were provided by KMCO₂ for the 19 producers in the study area:

- Quarterly Gas Production Rate
- Quarterly Water Production Rate
- Quarterly Oil Production Rate

Injection data were provided by KMCO₂ for the 3 producers converted to WAG injectors:

- Quarterly Water Injection Rate
- Quarterly Gas Injection Rate

The total production and injection rates of the study area are presented Figures 15 and 16. Production started in August 1949 inside the study area and is still active today. Water injection started in April 1961 and was then converted to WAG²³ in July 1973 inside the study area. WAG injection is still active today on the Northern Platform. Gas injection stopped in August 1996 inside the study area.

The reservoir model comprised 19 producers, but 3 were converted to water then to WAG injectors. Twelve (12) pseudo-injection wells were also implemented to reproduce proper boundary conditions. This is explained further in the next section. The model was run on Liquid Production Rate, with a minimum bottom-hole pressure of 28 psia. Injecting wells were controlled by gas and water injection rate. WAG injection consisted of water alternating with CO₂ injection. From the literature⁷, miscibility was not achieved in this area of the reservoir due to a reservoir pressure below minimum miscible pressure (MMP). Furthermore, by the time the model was built, no compositional data were available, thus another reason to build a black-oil model.

Because a black-oil model was used, proper CO₂ behavior could not be accurately reproduced. To address this issue:

- Injected gas composition was specified as CO₂: this allowed modeling accurate CO₂ flows inside the wellbore.
- Inside the reservoir, properties of a lean miscible gas were used for injected gas phase (only option available in black oil model).

This definitely had an impact on the recovery factor, but it ended up not being as critical as it will be presented in the results section. Figures 17 and 18 present respectively a planar section (layer 17) and a 3D view of the current reservoir model of porosity.

Reservoir Boundary Conditions

The first model built for the study area assumed no-flow boundary conditions, which was obviously not rigorous since the modeled study area is surrounded by producing and injecting wells. Hence, a volumetric method was used to evaluate fluxes entering (influx) and exiting (efflux) the study area.

This method was purely volumetric and used actual production and injection data from the wells within the study area. The difference between total water production and water injection rates was calculated, and the results are presented in Figure 19. This approach indicated strong influxes entering the study area, and also provided a good picture of the fluxes versus time. However, it did not define precisely the time of water breakthrough. Indeed, there is always a delay between the time the water is injected and the time it is recycled or reproduced. Therefore, some uncertainties were inherent to this method. To account for those uncertainties, water influxes were implemented but varied at the edge of the model.

Twelve (12) pseudo-injectors were implemented at the boundaries of the study area (3 injecting wells on each side). Water injection rate for each well was then calculated as follow: The model was subdivided in four areas, represented in Figure 20. For each quadrant, total water injection was subtracted from total water production. This defined a total water influx rate per quadrant, as presented in Figure 21. Since three injecting wells were present inside each quadrant, total water injection rate per quadrant was divided by three to get an injection rate for each injection well along the entire period of production. To

vary water influxes at the edge of the model, the water injection rate of each pseudo-injector was multiplied by a factor varying between 0.2 and 1. This factor was optimized during the history matching process.

History Matching Procedure

The automated history matching is an iterative technique utilizing two software programs, the global optimizer³⁰ (ClearVu) and a black-oil reservoir simulator²¹. The first step begins with a spreadsheet version of the simulator²¹ input file that is built in order to facilitate the variation of input parameters through the addition of formulas (Corey correlations for relative permeability curves, for example). Before the optimization process is started, the case is defined by generating possible ranges for uncertain input parameters (minima and maxima) as well as the total number of simulations to be run and the number of simulations per batch (also referred to as an iteration).

The current set of input parameter values is generated by the optimizer based on the probability distributions previously defined by the user. These parameter values are then inserted into the simulator input file in their appropriate locations and the spreadsheet is converted to a standard ASCII input file.

Simulations are executed one after the other and at the end of each iteration, the output data from each simulation is saved and compared to historical data. At this point, the corresponding error value is computed^{20,30}. These computed error values serve as objective (goodness-of-fit) function values and are evaluated by the optimizer, which produces a new set of input parameters. The next iteration can then be initialized. When several output parameters are to be matched, the objective function is computed separately for each parameter with the final error value being the sum (or some other combination) of the independent error values³⁰. The workflow of the process and the algorithm used by the optimizer are described in more detail in reference 20.

The optimizer uses an “evolution strategy”^{30,31} to reach optimum solutions. The basic idea of such strategy is to mimic biological evolution, also known as mutation-selection-mechanism (Darwinian Theory). Numerically, the great advantage of employing evolutionary strategy is that it is not necessary to calculate derivatives. Consequently, it is possible to deal with non-linear functions more easily than with any other optimization techniques. Although an evolutionary algorithm is a very general and robust optimization technique, it is possible in each specific case to make the optimization more efficient and converge faster by applying known domain knowledge and good parameter settings.

Some input parameters were unavailable for the study. Those parameters were varied during the history matching as were uncertain parameters. The porosity and permeability characterizations were developed in a grid that could work directly in the flow simulator¹⁹. Both the geostatistical characterizations and the reservoir flow simulations were conducted on the same Cartesian grid. Confidence in the porosity model developed with this grid definition was high, but it was suspected that the values of permeability populating the model grid-blocks could have been underestimated.

Therefore, the permeability characterization was varied quantitatively. This geostatistical characterization was kept the same in order to preserve geological trends and heterogeneities that were identified during the geostatistical process. But the entire characterization was multiplied by a factor varying between 1 and 5 that needed to be optimized during the history matching process. Hence, each value of permeability of the geostatistical model was multiplied by the same factor.

Additionally, as mentioned before, the factor multiplying water influxes at the edge of the model was also optimized. Table 5 presents the known or fixed parameters (and their corresponding values) inside the reservoir model. Likewise, Table 6 presents the 13 unknown or varying parameters that had to be optimized during the history matching.

The tactics used to achieve this history match were:

- Vary horizontal permeability
- Evaluate effects of vertical permeability variability
- Evaluate effects of changes in relative permeability
- Evaluate the effects of injection rate variability of the pseudo-wells at the edge of the model

History Matching Results

The dependent (history match) parameters were, for each individual producing well, Gas Production rate, Liquid Production Rate, and Water Production Rate. Average Reservoir Pressure was matched as well. One hundred and ninety eight (198) runs were necessary to achieve a good match and convergence of the parameters.

Figure 22 to Figure 38 present the comparison of the actual versus simulated gas, liquid and water production rates for each

individual well located in the center of the model. It is believed boundary conditions were properly reproduced for those wells. History matching results of outer wells are presented in Appendix A of reference 20. Figure 38 presents the actual versus simulated average reservoir pressure.

The modeling efforts resulted in a very good history match for the center wells in the study area. A good match was also obtained for the outer producing wells, and was achieved due to an optimized boundary effect. A good reservoir pressure match was also obtained, even though the implementation of effluxes would have helped to improve the pressure match between 1972 and 1988.

Overall, the match of liquid production rate was very well achieved. Matches of oil, gas and water production rates were satisfactory to very good. The average reservoir pressure match is also of good quality although it is slightly high between 1972 and 1988. Oil cut and gas production rate could be improved for wells 36-C3, 37-5, 37-6 and 59-1. Wells 36-C3, 37-5 and 37-6 produced too much oil compared to actual data. Since the reservoir pressure is above the bubble point pressure, too much gas is also produced (GOR=1,000 scf/bbl). Well 59-1 doesn't produce enough oil compared to actual data, hence not enough gas. Wells 36-C3, 37-5 and 37-6 are located in areas where permeability and porosity are particularly heterogeneous from one layer to another. Well 59-1 is located in a high porosity zone.

As explained earlier, only one rock type (one set of relative permeability curves for oil-water and gas-liquid) was used in this model. The match of production rates for all wells could probably be improved if several rock types were defined inside the model, so that each rock type could be assigned different relative permeability curves.

Additionally, only water influxes have been simulated at the edge of the model. Water efflux and oil/gas fluxes have not been simulated. The match of the average reservoir pressure could probably be improved if flux for all phases were implemented, allowing some efflux to occur, hence decreasing the average reservoir pressure.

Table 7 presents the optimized parameter values. Average porosity from the geostatistical characterization was 8.5%. Values ranging from 7 to 10% were found in the literature. Average permeability defined by history matching is 2.74 mD multiplied by a factor of 3, so 8.22 mD. Values of average permeability found in the literature are around 15 mD. The injection ratio defining water influxes converged at 0.8. This is not far from the predicted injection rate.

A 3D view of the residual oil saturation at the end of the producing period is presented in Figure 39. Based on those irreducible water and residual oil saturations, the recovery factor from the reservoir model is equal to 46%. In published literature³² a maximum of 39% was reported for the entire SACROC unit. The recovery factor is likely overestimated in our model due to the injection of miscible gas in the black-oil model, when immiscibility injection should occur.

Conclusions:

1. An integrated methodology combining clustering analysis techniques, geostatistical methods and evolutionary strategy technologies was developed and successfully tested in the Pennsylvanian-Permian reef carbonates (Cisco and Canyon Formations) of a subregion of the SACROC Unit, Horseshoe Atoll, Permian Basin, Texas.
2. This approach was initially constituted by a two-step pattern recognition procedure (soft-computing) combined with the application of geostatistical algorithms. The soft-computing procedure permitted the efficient generation of core-scale P&P profiles and rock types at well locations where no core data existed populating this way all wells inside the studied area. These core-scale estimates of P&P and rock types facilitated direct application of geostatistical methods to build 3D reservoir models.
3. Clustering analyses indicated that the SACROC carbonate section can be divided into a suite of closely-related flow units that have a "good" RQ (average porosity ~ 11-13 %) and into a suite of closely-related flow units that have a "poor" RQ (average porosity generally < 5 %). As interpreted from clustering analysis output, the contacts between these good and poor suites is generally rather sharp, as opposed to the generally gradational contacts that exist among the several flow units that comprise the good and poor suites.
4. Different scales of variability can be seen in variograms of core porosity and permeability (actual and estimated values). The vertical variogram analysis of core porosity and permeability (actual and estimated values) indicated spatial behaviors associated with geologic cyclicity. Cyclicity could not be appreciated in horizontal variograms.
5. Both variography studies, vertical and horizontal, conducted to variogram models using an isotropic nugget structure and two structures reflecting an intermediate and a global scale mainly associated to complex patterns of sediment

deposition of the reservoir, and constructional characteristics of the SACROC limestone reef (structural factors).

6. From the qualitative and quantitative point of views, a 3D geostatistical porosity model highly trustworthy was developed with this combined methodology. A highly reliable permeability model was generated from the qualitative viewpoint (identification and characterization of geological trends and realistic heterogeneities); however, estimated permeability values were considered possibly undervalued.
7. An assisted history match was successfully achieved using evolutionary algorithms for global optimization. This history match was based on the matching of oil, gas and water production rates, and the average reservoir pressure. The match was accomplished by manipulating thirteen uncertain design parameters which included two formation properties, other ten variables related with the corresponding relative permeability curves, and one variable linked to the reservoir production.
8. History match results confirmed that the 3D reservoir models of P&P constructed applying the combined reservoir characterization approach (advanced pattern recognition techniques and geostatistical algorithms) were legitimate representations of the spatial distribution of these parameters in the reservoir. In addition, results confirmed initial assumption that the developed permeability model, despite of capturing correctly geological trends and heterogeneities of Canyon Reef reservoir (SACROC field) presented slightly underestimated values.
9. A very good history match was attained for the center wells performance in the study area; a good match was also achieved for the outer producing wells and the average reservoir pressure. These achievements were thanks to the setting up of proper boundary conditions that described the flow behavior at the boundary of the analyzed region. Overall, the match of liquid production rate was very well achieved. Matches of oil, gas and water production rates were from satisfactory to very good. The average reservoir pressure match was also of good quality although slightly high between years 1972 and 1988.
10. The implementation of twelve pseudo-injectors at the boundaries of the study area reproduced accurately water influxes at the edge of the model. The use of a multiplicative factor for water influxes at the edge of the model was determinant in this process. This factor, varied between 0.2 and 1, converged at 0.8 which was close to calculated injection rates using differential water volume technique (Method 2).
11. The simple black oil model developed here was sufficient to capture the reservoir behavior of SACROC Unit, Canyon Reef Formation due to simulated oil-water relative permeability curves matched perfectly actual core measurements, and the recovery factor from the simulated reservoir model was equal to 46% (a maximum of 39% has been reported in literature).
12. The direct application of conventional geostatistical algorithms in this work is favored by the application of advanced pattern recognition techniques that provide likely rock types and reliable estimates of P&P (with high vertical resolution) at all well locations. Reciprocally, the utilization of geostatistical algorithms allows the three-dimensional extension of those local results derived from the application of the clustering methodology. This “symbiotic” interaction between these two mathematical approaches strengthens their corresponding possibilities of applicability offering a significant advance over their individual uses, and other conventional methodologies.
13. The addition of optimization methods (for assisted history matching) to the combined soft-computing/geostatistical approach (utilized for reservoir characterization purposes) constitutes a powerful triad of mathematical techniques ideally suited for addressing reservoir integrated studies, with the capacity of facing these complex tasks more rapidly and efficiently than using traditional methodologies.

Acknowledgments:

The authors thank Kinder Morgan CO2 Company, L.P. for permission to publish this paper. Acknowledgments are also extended to Michael Raines for his helpful comments. This work was supported by U.S Department of Energy under project DE-FC26-04NT15514.

Nomenclature:

AI_log = Acoustic Impedance from RHOB and DT
CMP = Cumulative Mode Probability

DT	=	delta time
GR	=	gamma ray
K0	=	permeability along master orientation line
K90	=	permeability at 90 degrees from K0 line
KV	=	vertical permeability
NPHI	=	neutron porosity
OOIP	=	Original Oil In Place
P&P	=	porosity and permeability
RHOB	=	bulk density
RQ	=	reservoir quality
SGS	=	Sequential Gaussian Simulation
WAG	=	Water Alternating Gas

References:

1. Perlovsky, L.I. and McManus, M.M.: "Maximum Likelihood Neural Networks for Sensor Fusion and Adaptive Classification", *Neural Networks*, Vol. 4, pp.89-102, 1991.
2. Perlovsky, L. I.: "Computational concepts in classification: Neural Networks, Statistical Pattern Recognition, and Model Based Vision", *Journal of Mathematical Imaging and Vision*, v 4(1), p. 81-110, 1994.
3. Eslinger, E.: "GAMLS (Geologic Analysis via Maximum Likelihood System). User's Manual", ericgeoscience.com, Eric Geoscience, Inc., 2000.
4. Eslinger, E., Burdick, B., and Cooper, J.: "Reservoir Characterization Using a Probabilistic Clustering Procedure", (in progress), 2007.
5. Raines, M., Dobitz, J.K., and Wehner, S.C.: "A Review of the Pennsylvanian SACROC Unit", paper presented at 2001 West Texas Geological Society Fall Symposium, Midland, TX, Oct. 24-25.
6. Vest, E. L. Jr.: "Oil Fields of Pennsylvanian-Permian Horseshoe Atoll, West Texas" in Halbouty, Michael T. (ed.) *Geology of Giant Petroleum Fields*, AAPG Memoir N 14. American Association of Petroleum Geologists, Tulsa Oklahoma, pp. 185-203, 1970.
7. Raines, M.: Personal Communication, 2007.
8. Gonzalez, R.J., Reeves, S.R., and Eslinger, E.: "Predicting Porosity and Permeability for the Canyon Formation, SACROC Unit (Kelly-Snyder Field), Using the Geologic Analysis via Maximum Likelihood System", Topical Report prepared for U.S. Department of Energy, DE-FC26-04NT15514, September 2007.
9. Raines, M., and Helms, W.: "Sample Size Impact on Permeability Values and Implications for Reservoir Models", *West Texas Geological Society's Bulletin*, vol. 46, N 4, March 2007.
10. Eslinger, E., "Procedures for Lithology Characterization and Probabilistic Upscaling (Curve "Blocking") Using Petrophysical and Core Data", AAPG National Meeting (poster session), Long Beach, CA, April 3 2007.
11. Gonzalez, R.J., Reeves, S.R., Eslinger, E., and Garcia, G.: "Development and Application of an Integrated Clustering/Geostatistical Approach for 3D Reservoir Characterization, SACROC Unit, Permian Basin", paper SPE 111453-PP presented at the 2007 SPE/EAGE Reservoir Characterization and Simulation Conference. Abu Dhabi, U.A.E., 28-31 October 2007.
12. Deutsch, C.V.: "Geostatistical Reservoir Modeling", first edition, Oxford University Press, 2002.
13. Deutsch, C.V., and Journel, A.G.: "GSLIB. Geostatistical Software Library and User's Guide", second edition, Oxford University Press, 1998.
14. Goovaerts, P.: "Geostatistics for Natural Resources Evaluation", first edition, Oxford University Press, 1997.
15. Yarus, J.M. and Chambers, R.L.: "Practical Geostatistics—An Armchair Overview for Petroleum Reservoir Engineers". *JPT* (November 2006) 78.
16. Remy, N.: "SGEMS: The Stanford Geostatistical Earth Modeling Software. User's Manual", http://sgems.sourceforge.net/doc/sgems_manual.pdf, May 2004.
17. Gringarten, E., and Deutsch, C.V.: "Variogram Interpretation and Modeling", *Mathematical Geology*, Vol. 33, N 4, 2001.
18. J.P. Benkendorfer, J.P., Deutsch, C.V., LaCroix, P.D., Landis, L.H., Al-Askar, Y.A, Al-AhdulKafim, A.A., and Cole, J.: "Integrated Reservoir Modelling of a Major Arabian Carbonate Reservoir", paper SPE 29869 presented at the 1995 SPE Middle East Oil Show, Bahrain, March 11-14.
19. Gonzalez, R.J., and Reeves, S.R.: "Geostatistical Reservoir Characterization of the Canyon Formation, SACROC Unit, Permian Basin", Topical Report prepared for U.S. Department of Energy, DE-FC26-04NT15514, September 2007.

20. Schepers, K., Gonzalez, R.J., and Reeves, S.R.: "Optimized Reservoir History Matching Simulation of Canyon Formation, SACROC Unit, Permian Basin", Topical Report prepared for U.S. Department of Energy, DE-FC26-04NT15514, September 2007.
21. "IMEX. Advanced Oil/Gas Reservoir Simulator. 2007 User's Guide", Computer Modelling Group Ltd., 2007.
22. Isaaks, E.H., and Srivastava, R.M.: "An Introduction to Applied Geostatistics", first edition, Oxford University Press, 1989.
23. Kane, A.V.; "Performance Review of a Large-Scale CO₂-WAG Enhanced Recovery Project, SACROC Unit, Kelly-Snyder Field", SPE 7091, presented at the SPE/AIME Fifth Symposium on Improved Methods for Oil Recovery, Tulsa, OK, April 16-19, 1978.
24. Allen, H.H., Thomas, J.B.; "Pressure Maintenance in SACROC Unit Operations", SPE 1259-G, presented at the Permian Basin Section Oil Recovery Conference, Midland, TX, May 7-8, 1959.
25. Allen, H.H., LaRue, C.R.; "SACROC Unit Operations", SPE 829-G, presented at Permian Basin Oil Recovery Conference, Midland, TX, April 18-19, 1957.
26. Graue, D. J., Blevins, T.R.; "SACROC Tertiary CO₂ Pilot Project", SPE 7090, presented at the Fifth Symposium on Improved Methods for Oil Recovery of the Society of Petroleum Engineers of AIME, Tulsa, OK, April 16-19, 1978.
27. Langston, M.V., Hoadley, S.F., Young, D.N.; "Definitive CO₂ Flooding Response in the SACROC Unit", SPE 17321, prepared for the SPE/DOE Enhanced Oil Recovery Symposium, Tulsa, OK, April 17-20, 1988.
28. Dicharry, R.M., Perryman, T.L., Ronquille, J.D.; "Evaluation and Design of a CO₂ Miscible Flood Project – SACROC Unit, Kelly-Snyder Field", SPE 4083, prepared for the Journal of Petroleum Technology, pg. 1309 - 1318, November, 1973.
29. Brummett, W.M., Jr., Emanuel, A.S., Ronquille, J.D.; "Reservoir Description by Simulation at SACROC – A Case History", SPE 5536, prepared for the Journal of Petroleum Technology, pg. 1241 – 1255, October, 1976.
30. Development of Optimized History-Matched Models for Coalbed Methane Reservoirs. Oudinot, A., Sultana, A., Gonzalez, R.J., Reeves, S.R., and Wörmann, M.
31. Baeck, T., Fogel, D.B., Michalewicz, Z.; "Handbook of Evolutionary Computation"; Oxford University Press, New York, Oxford, 1997.
32. Langston, M.V., Hoadley, S.F., Young, D.N.; "Definitive CO₂ Flooding Response in the SACROC Unit", SPE 17321, prepared for the SPE/DOE Enhanced Oil Recovery Symposium, Tulsa, OK, April 17-20, 1988.

Table 1: Formation, Fluid and Well Properties of the Reservoir Model

Parameter	Units	Value	Reference Depth/Pressure
Formation Properties			
Initial Pressure	psia	3137	at 4300ft TVDSS (actual data)
Initial Temperature	F	132	at 4300ft TVDSS (actual data)
Initial Water Oil Contact	FT	4500	TVDSS (actual data)
Rock Compressibility	1/psi	5.60E-06	at 3137 psia (actual data)
Fluid Properties			
Bubble Point Pressure	psi	1850	at 4300ft TVDSS (actual data)
Oil Compressibility	1/psi	7.00E-05	at 1850 psia (Ramey's correlation ¹⁵)
Oil Density	API	37.2	at STC (actual data and Mc Cain's correlation ¹⁶)
Gas Gravity	-	0.67	at STC (Standing and Katz's correlation ¹⁷)
Water Compressibility	1/psi	2.90E-06	at 1850 psia (Dodson and Standing's correlation ¹⁸)
Water Density	-	62.3	(Earlougher, R.C. ¹⁹)
Water FVF	RB/STB	1.013	(Rowe and Chou's correlation ²⁰)
Water Viscosity	cp	0.51	(actual data and Matthews and Russell's correlation ²¹)
Relative Permeability Relationships			
Krliq	-	1	assumed
Well Parameters			
Skin Producers	-	-1	assumed
Skin injectors	-	-1	assumed

Table 2: Available Formation Properties

Parameter	Units	Value	Source
Initial Pressure	psia	3137	SPE 4083 ⁴ , 5536 ⁵ , 1259-G ⁹ , 829G ¹⁰ , 17321 ¹²
Temperature	F	132	SPE 4083 ⁴ , 5536 ⁵ , 1259-G ⁹ , 829G ¹⁰ , 17321 ¹²

Table 3: Available Fluid Properties

Parameter	Units	Value	Source
Oil Gravity (STC)	API	41	SPE 17321 ¹²
Bubble Point Pressure	psi	1850	SPE 4083 ⁴ , 5536 ⁵ , 1259-G ⁹ , 829G ¹⁰ , 17321 ¹²
Water Viscosity	cp	0.51	SPE 4083 ⁴ , 5536 ⁵ , 1259-G ⁹ , 829G ¹⁰ , 17321 ¹²

Table 4: Available PVT Data

Pressure	Rs	Bo	Oil Viscosity
(psia)	(cuft/bbl)	(RB/STB)	(cp)
1850	1000	1.55	0.35
3137		1.523	

Note: Data from Table 3 come from literature^{4, 5, 11, 12}

Table 5: Fixed Parameters During History Matching

Parameter	Units	Value	Source
Formation Properties			
Average Thickness	ft	900	Geostatistical Characterization ^{2,3}
Initial Pressure	psia	3137	SPE 4083 ⁴ , 5536 ⁵ , 1259-G ⁹ , 829G ¹⁰ , 17321 ¹²
Temperature	F	132	SPE 4083 ⁴ , 5536 ⁵ , 1259-G ⁹ , 829G ¹⁰ , 17321 ¹²
Average Porosity	%	8.5	Geostatistical Characterization ^{2,3}
Rock Compressibility	1/psi	5.60E-06	Correlation
Fluid Properties			
Oil Gravity	API	41	SPE 17321 ¹²
Bubble Point Pressure	psi	1850	SPE 4083 ⁴ , 5536 ⁵ , 1259-G ⁹ , 829G ¹⁰ , 17321 ¹²
Gas Gravity	-	0.7	Assumed
Water Density	-	62	Assumed
Water Formation Volume Factor	RB/STB	1.013	Assumed
Water Compressibility	1/psi	2.90E-06	Correlation
Water Viscosity	cp	0.51	SPE 4083 ⁴ , 5536 ⁵ , 1259-G ⁹ , 829G ¹⁰ , 17321 ¹²
Relative Permeability Relationships			
Maximum Corey Kr liquid	-	1	assumed
Well Parameters			
Skin Producers	-	-1	assumed
Skin injectors	-	-1	assumed

Table 6: Varying Parameters During History Matching

Parameter	Units	Minimum	Maximum	Source
Formation Properties				
Permeability Multiplier	-	1	5	Geostatistical Characterization ^{2,3}
Vertical Permeability Ratio	-	0.01	1	
Relative Permeability Endpoints				
Irreducible Water Saturation	-	0.10	0.22	KMCO ₂
Residual Oil Saturation	-	0.20	0.30	KMCO ₂
Maximum Kr water (oil-water system)	-	0.40	1.00	KMCO ₂
Maximum Kr oil (oil-water system)	-	0.40	0.90	KMCO ₂
Kro Corey's Exponent (oil-water system)	-	1	4	KMCO ₂
Krw Corey's Exponent (oil-water system)	-	1	4	KMCO ₂
Residual gas Saturation	-	0.01	0.1	KMCO ₂
Maximum Krg (gas-liquid system)	-	0.1	0.7	KMCO ₂
Krg Corey's Exponent (gas-liquid system)	-	1	4	KMCO ₂
Krliquid Corey's Exponent (gas-liquid system)	-	1	4	KMCO ₂
Production Data				
Injection Rate Ratio	-	0.2	1	Calculations

Table 7: Optimized Parameters Obtained for the Match

Parameter	Units	Minimum	Maximum	Optimized	Source
Formation Properties					
Permeability Multiplier	-	0.5	5	3	Geostatistical Characterization ^{2,3}
Vertical Permeability Ratio	-	0.01	1	0.9	
Relative Permeability Endpoints					
Irreducible Water Saturation	-	0.10	0.22	0.21	KMCO ₂
Residual Oil Saturation	-	0.20	0.30	0.24	KMCO ₂
Maximum Kr water (oil-water system)	-	0.40	1.00	0.85	KMCO ₂
Maximum Kr oil (oil-water system)	-	0.40	0.90	0.86	KMCO ₂
Kro Corey's Exponent (oil-water system)	-	1	4	3.5	KMCO ₂
Krw Corey's Exponent (oil-water system)	-	1	4	1.2	KMCO ₂
Residual gas Saturation	-	0.01	0.1	0.09	KMCO ₂
Maximum Krg (gas-liquid system)	-	0.1	0.7	0.66	KMCO ₂
Krg Corey's Exponent (gas-liquid system)	-	1	4	1.7	KMCO ₂
Krliquid Corey's Exponent (gas-liquid system)	-	1	4	2	KMCO ₂
Production Data					
Injection Rate Ratio	-	0.2	1	0.8	Calculations

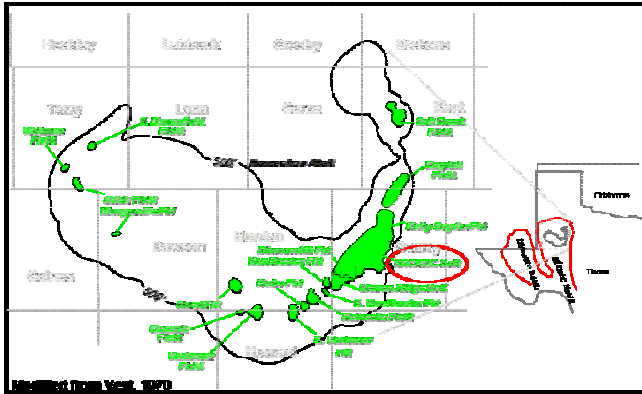


Figure 1: Location of the SACROC Unit, Permian Basin.

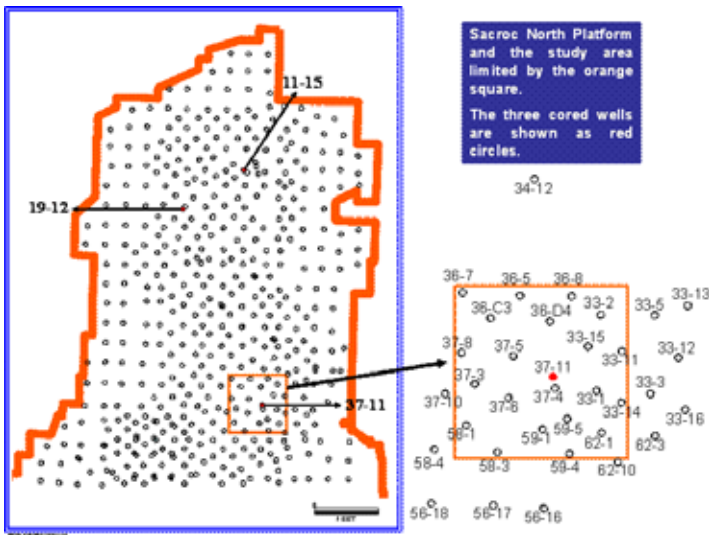


Figure 2: SACROC North Platform. Location of the Characterized Area

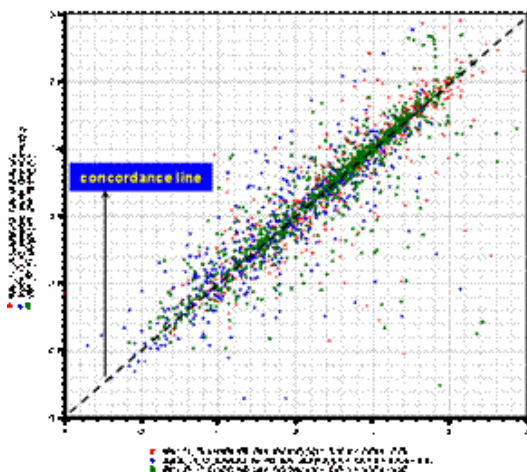


Figure 3: Cross Plot of $\log_{10}(K_0)$ vs. $\log_{10}(K_{90})$: Well 11-15 in Red; Well 19-12 in Blue; Well 37-11 in Green.

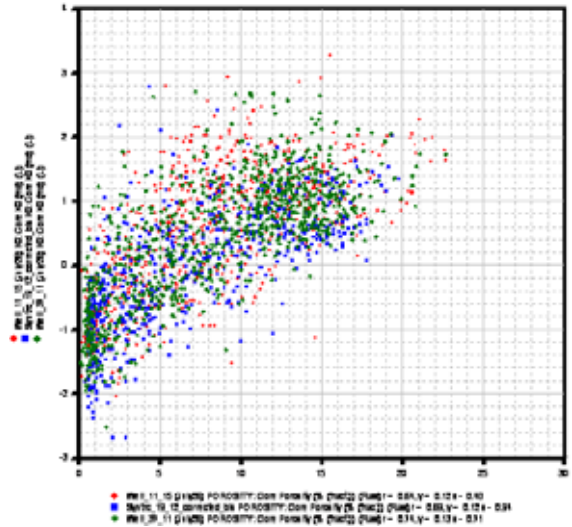


Figure 4: Cross plot of $\log_{10}(K_0)$ vs. porosity. Well 11-15 in red; well 19-12 in blue; well 37-11 in green.

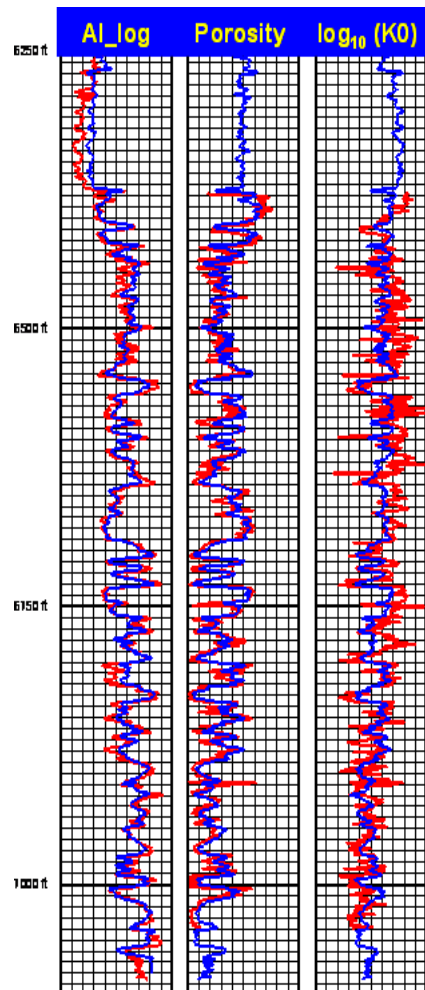


Figure 5: AI_log (1st track), Porosity (2nd track) and $\log_{10}(K_0)$ (3rd track) for Testing Hold-out Cored Well 11-15. Actual Parameter Values in red; Predicted Values in Blue.

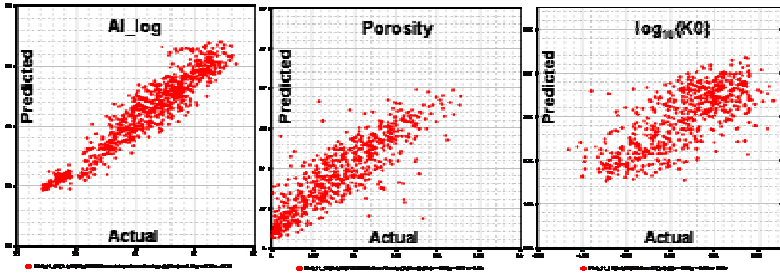


Figure 6: Cross Plots of Predicted vs. Actual Values for AI_log (left); Porosity (center); log₁₀(K0) (right). Ranges: AI_log [20, 60]; Porosity [0.0, 0.3]; log₁₀(K0) [-2.75, 2.75]

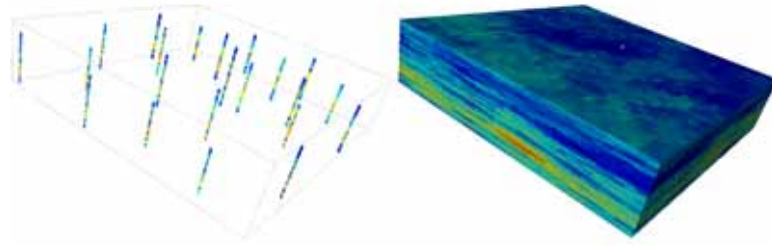


Figure 8: Averaged Porosity Model and Well Locations

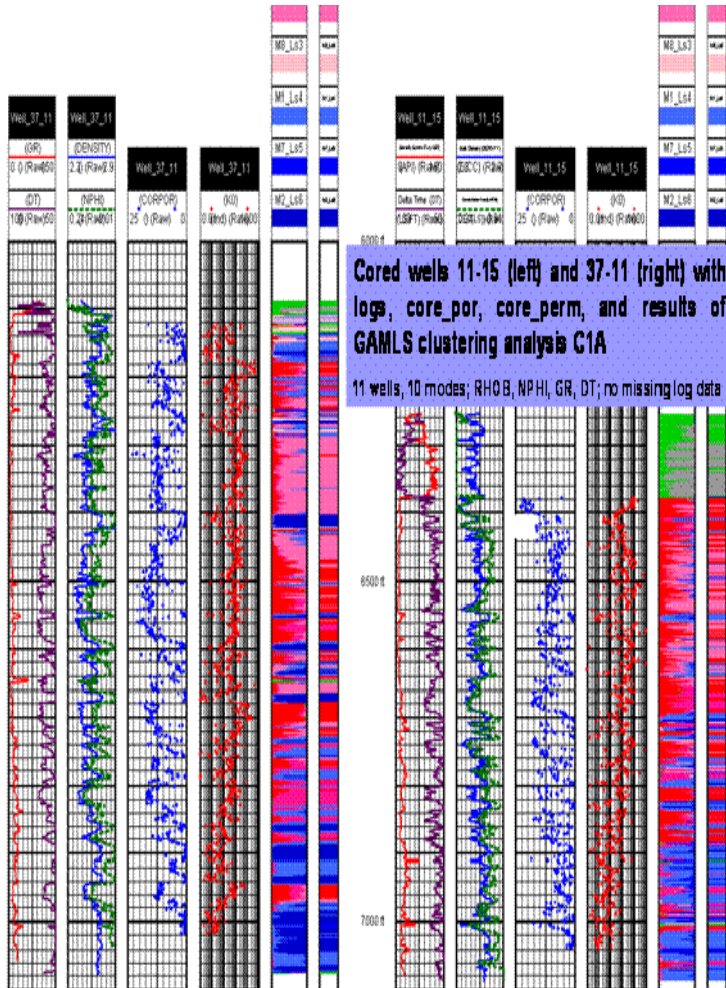


Figure 7: Tracks for cored wells 11-15 (left) and 37-11 (right). GR and DT logs (1st track), RHOB and NPHI logs (2nd track), actual porosity (3rd track), actual log₁₀(K0) (4th track), and rock types results of clustering C1A (5th track).

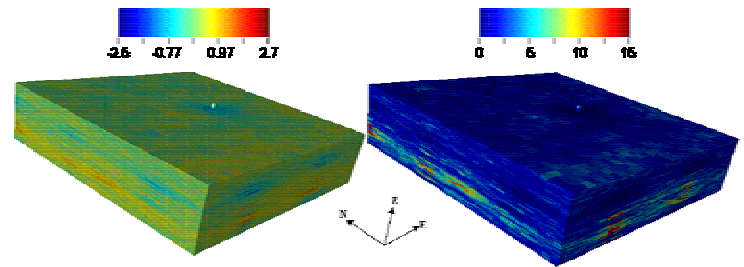


Figure 9: Averaged Logarithm of Permeability Model (left) and Permeability Model (right).

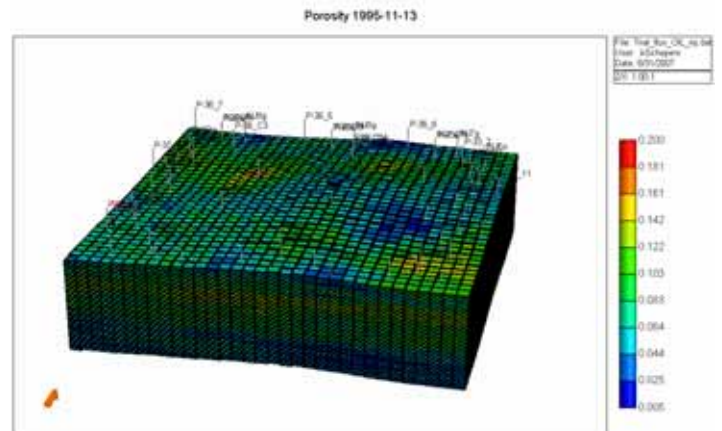


Figure 10: Porosity Model of the Study Area

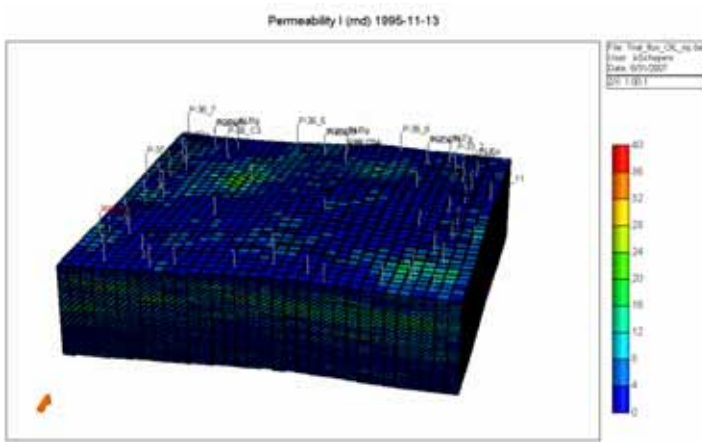


Figure 11: Horizontal Permeability Model of the Study Area

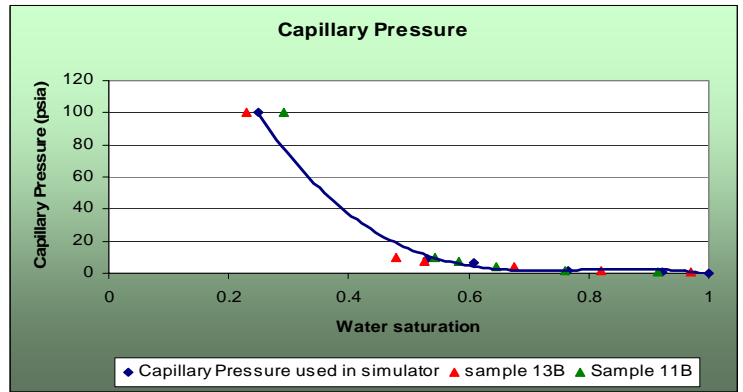


Figure 14: Capillary Pressure Curves Used in the Simulation

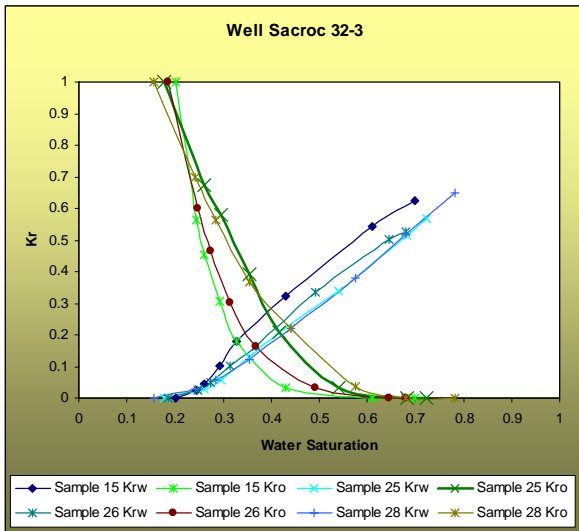


Figure 12: Oil-Water Relative Permeability Curves, Well 32-3

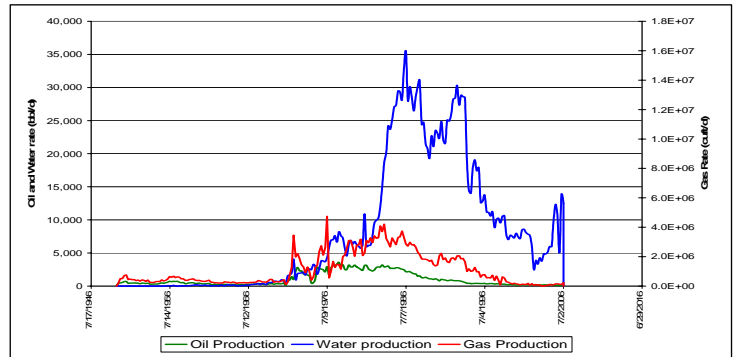


Figure 15: Production Rates for the Modeled Study Area

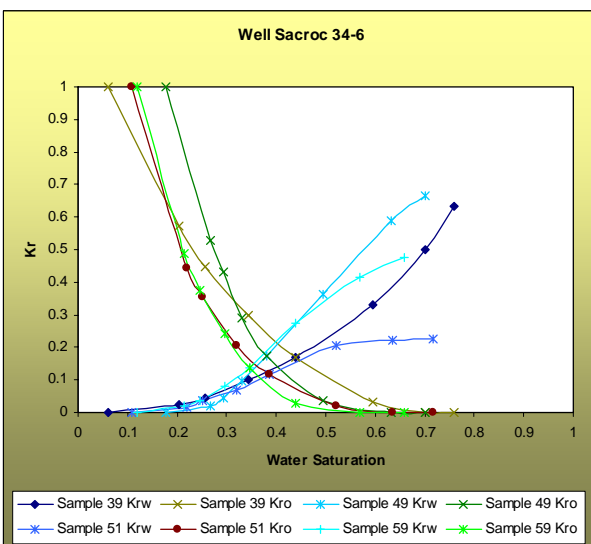


Figure 13: Oil-Water Relative Permeability Curves, Well 34-6

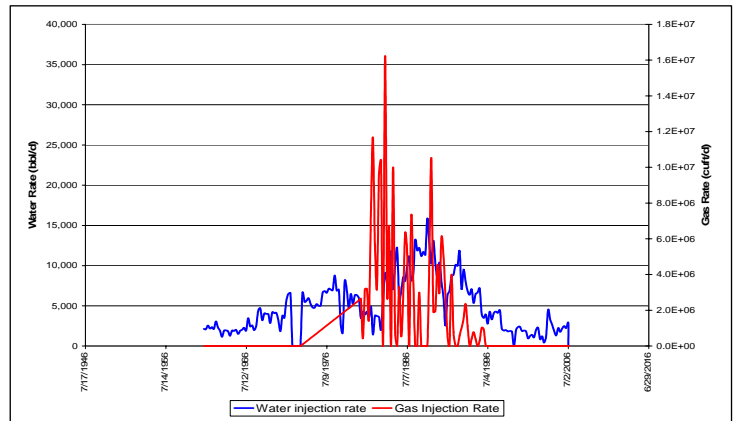


Figure 16: Injection Rates for the Modeled Study Area

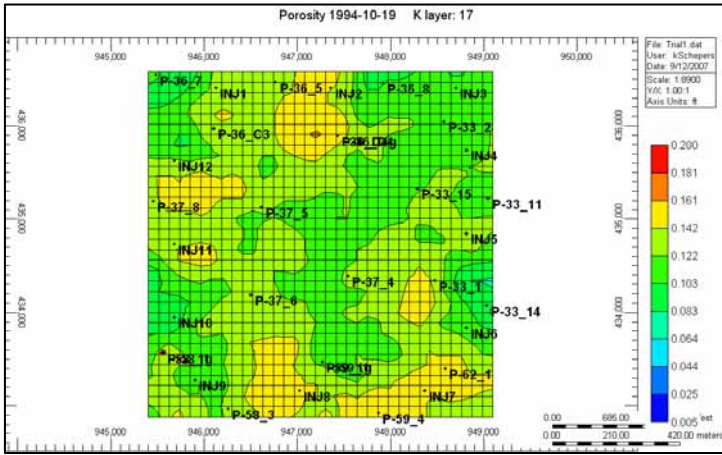


Figure 17: Study Area Reservoir Model - Top View

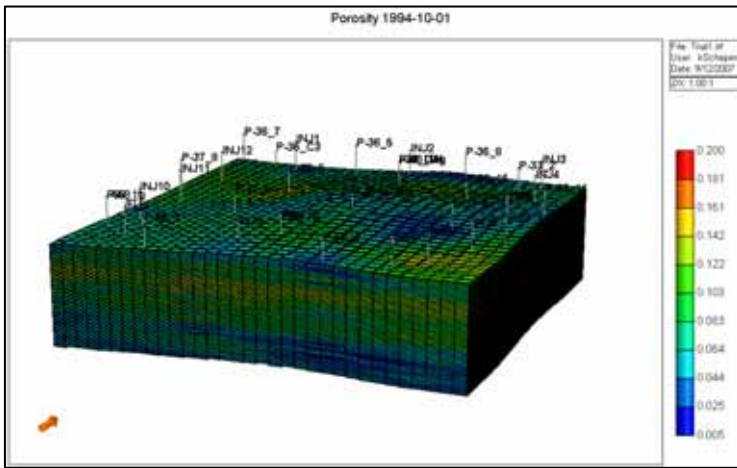


Figure 18: Study Area Reservoir Model - 3D View

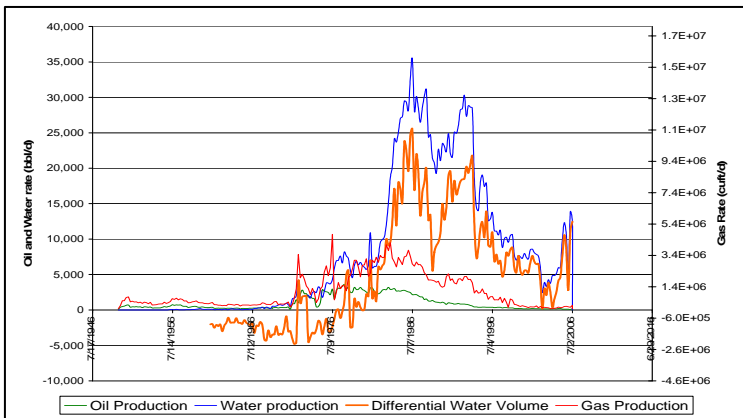


Figure 19: Differential Water Volume for the Model (Water Production - Water Injection)

Note: Differential Water Volume = Total Water Production Rate – Total Water Injection Rate The orange curve represents the difference between water production and injection versus

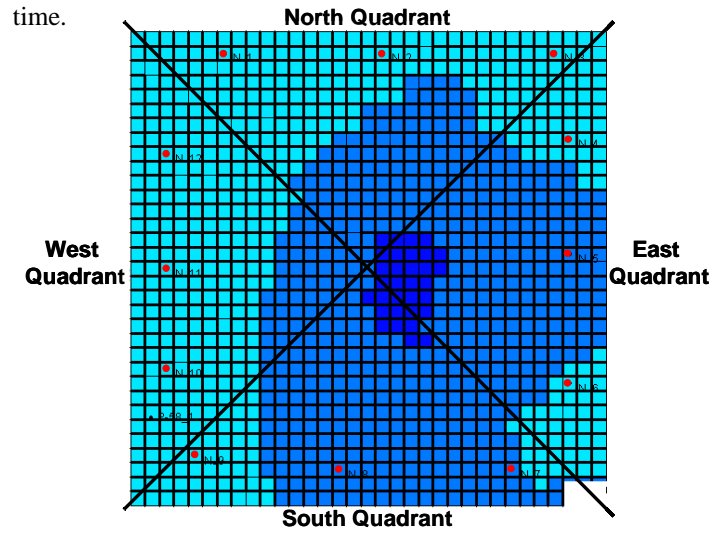


Figure 20: Location of the 12 Pseudo-Injectors (in Red) Inside the Four Quadrants of the Study Area

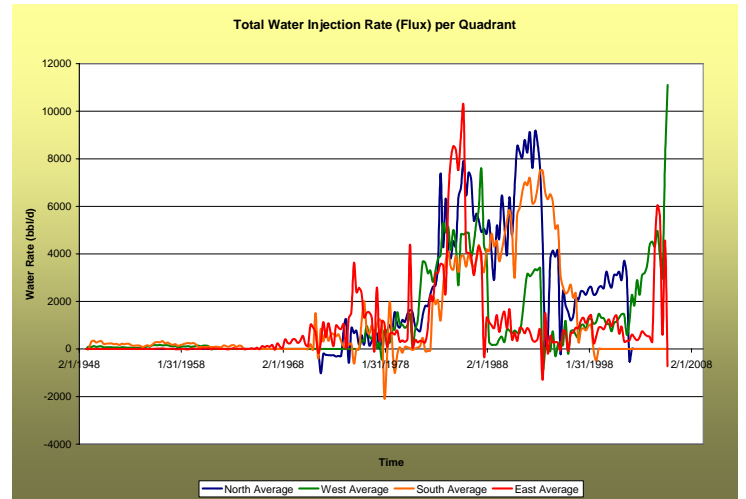


Figure 21: Water Flux per Quadrant (from Method 2)

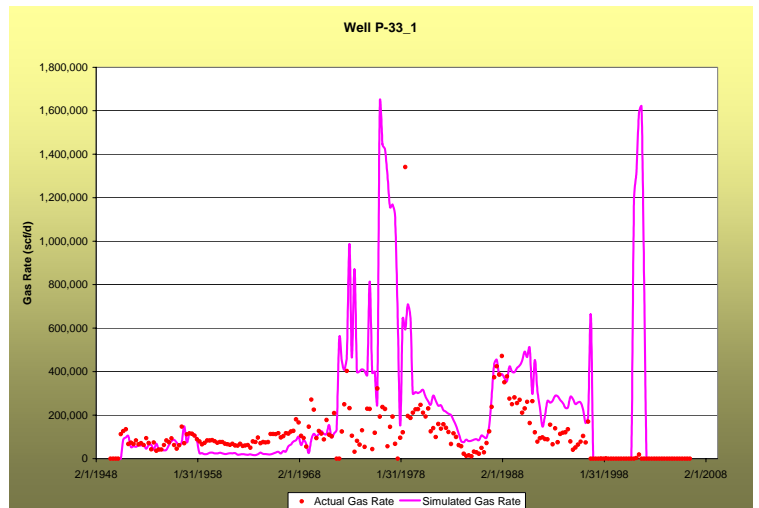


Figure 22: History Match of Gas Rate, Well P-33-1

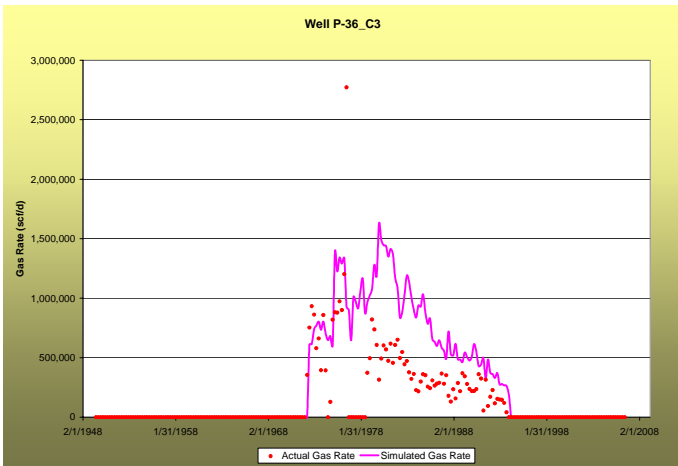


Figure 23: History Match of Oil and Water Rates, Well P-33-1

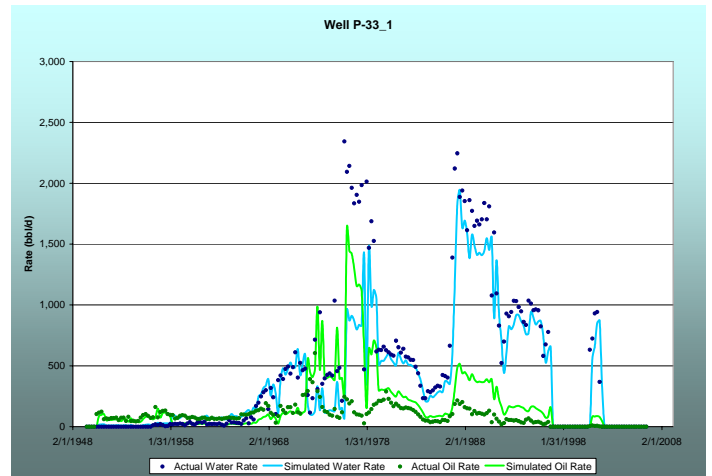


Figure 26: History Match of Gas Rate, Well P-36-C3

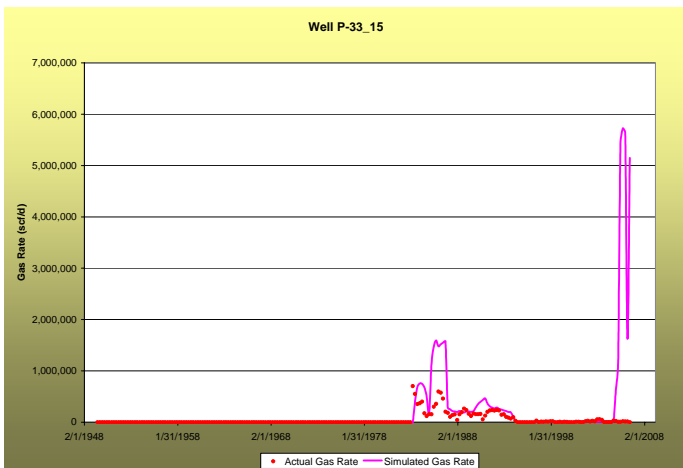


Figure 24: History Match of Gas Rate, Well P-33-15

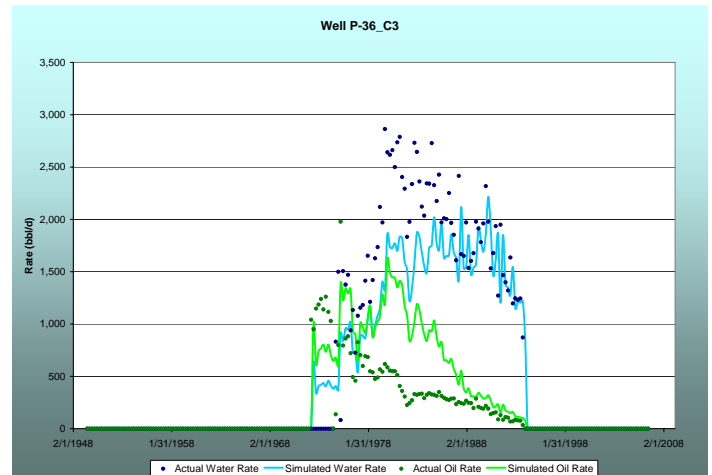


Figure 27: History Match of Oil and Water Rates, Well P-36-C3

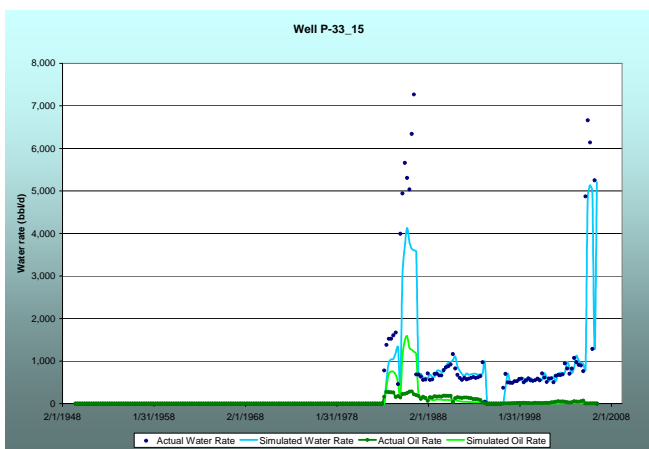


Figure 25: History Match of Oil and Water Rates, Well P-33-15

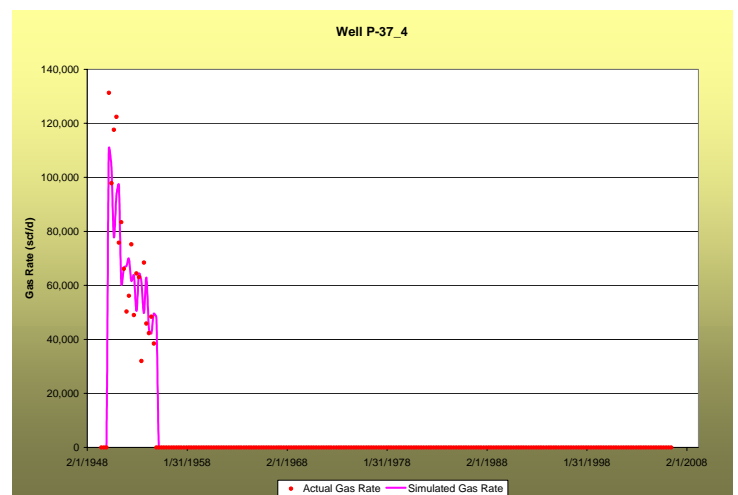


Figure 28: History Match of Gas Rate, Well P-37-4

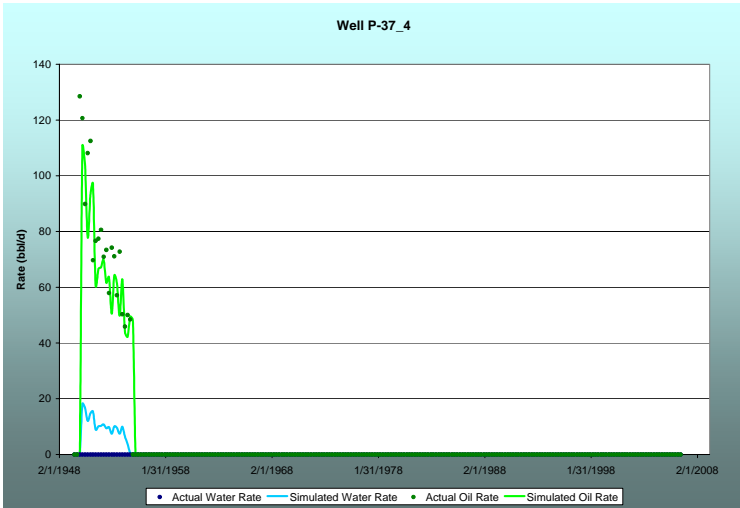


Figure 29: History Match of Oil and Water Rates, Well P-37-4

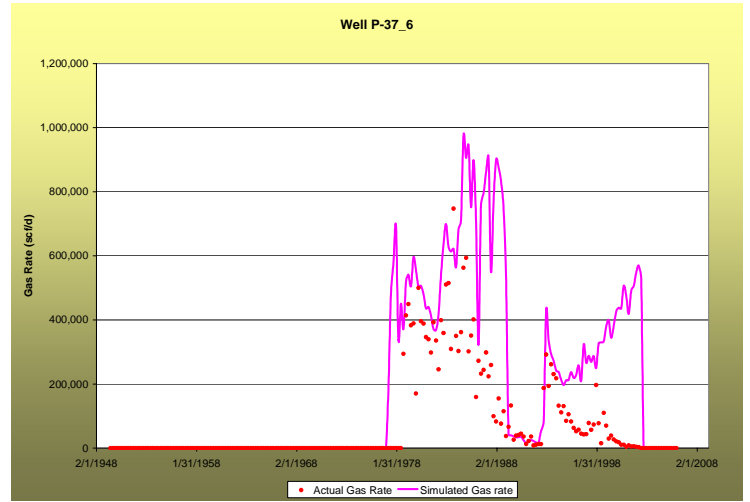


Figure 32: History Match of Gas Rate, Well P-37-6

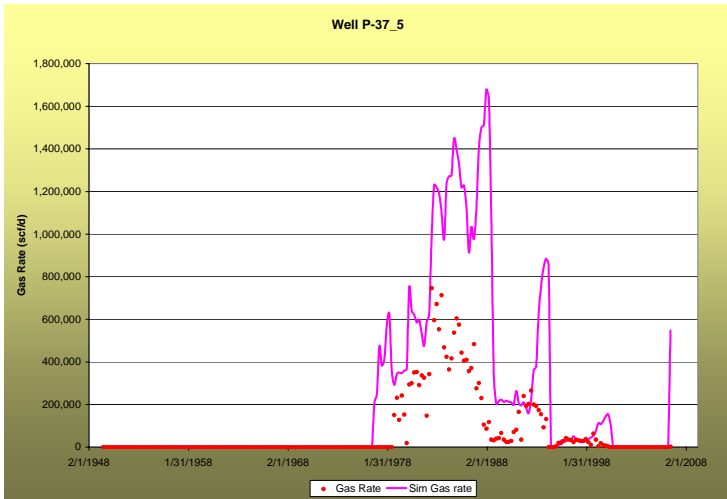


Figure 30: History Match of Gas Rate, Well P-37-5

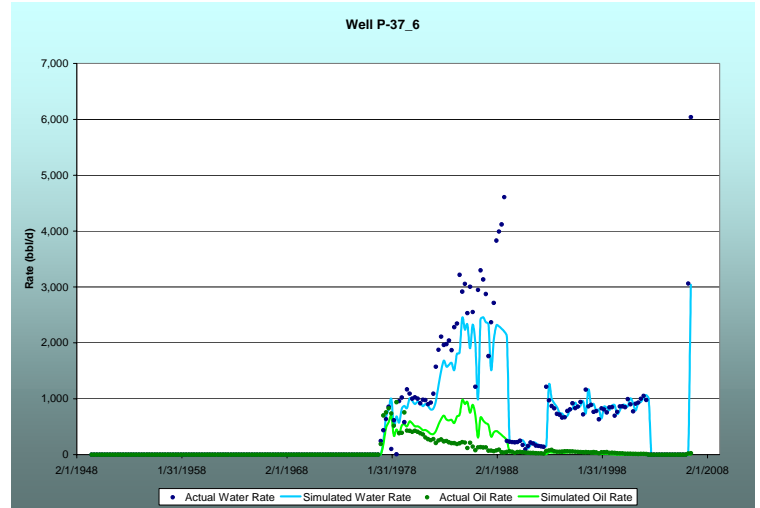


Figure 33: History Match of Oil and Water Rates, Well P-37-6

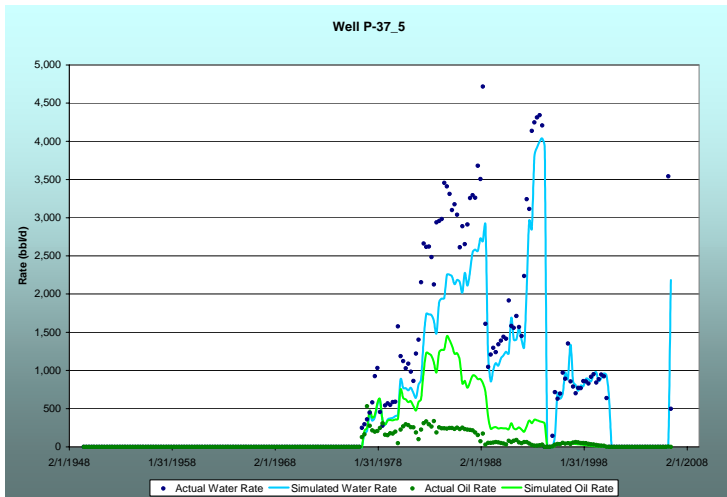


Figure 31: History Match of Oil and Water Rates, Well P-37-5

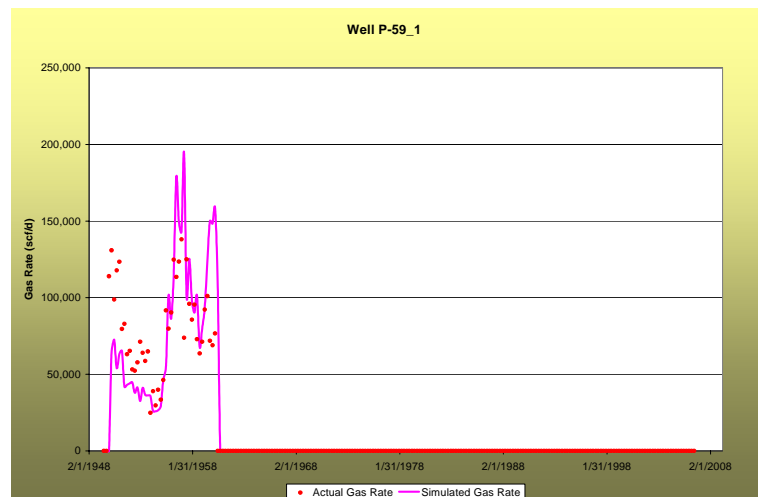


Figure 34: History Match of Gas Rate, Well P-59-1

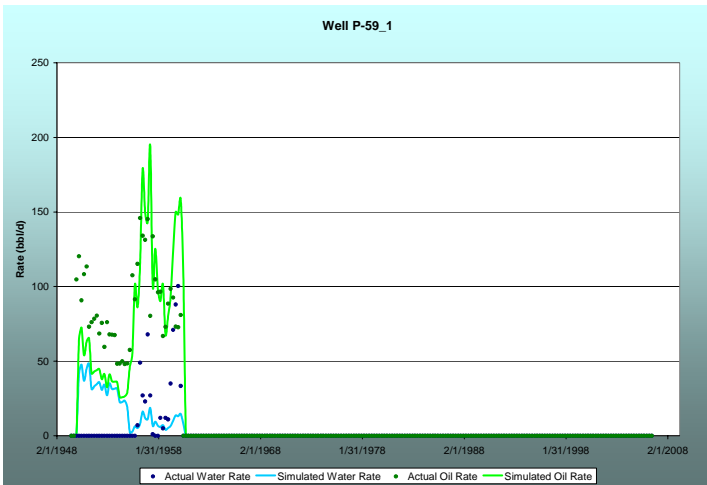


Figure 35: History Match of Oil and Water Rates, Well P-59-1

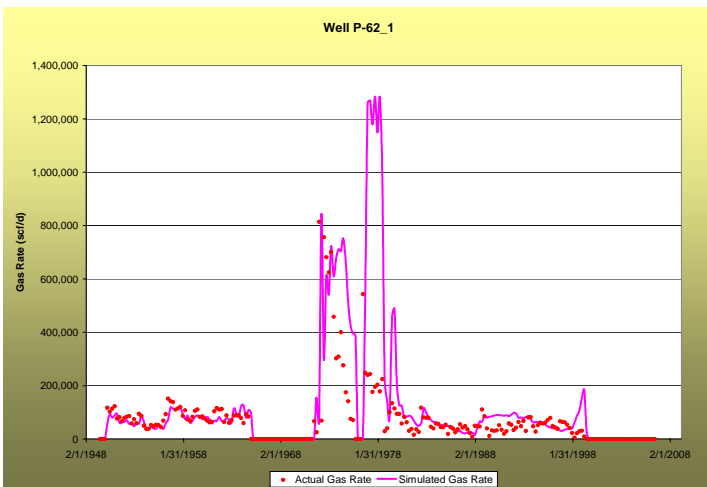


Figure 36: History Match of Gas Rate, Well P-62-1

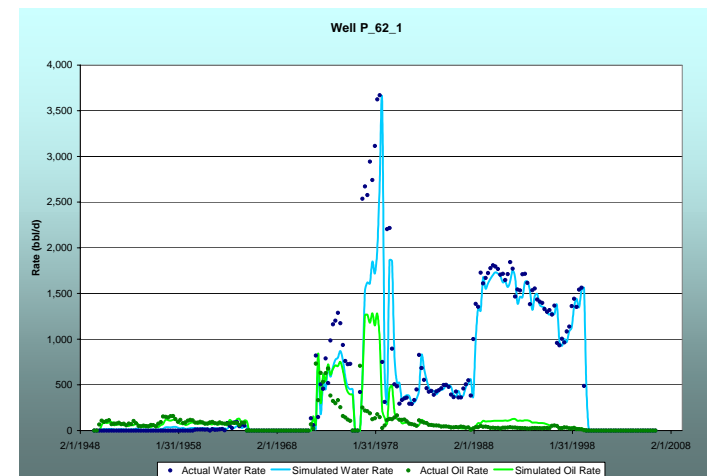


Figure 37: History Match of Oil and Water Rates, Well P-62-1

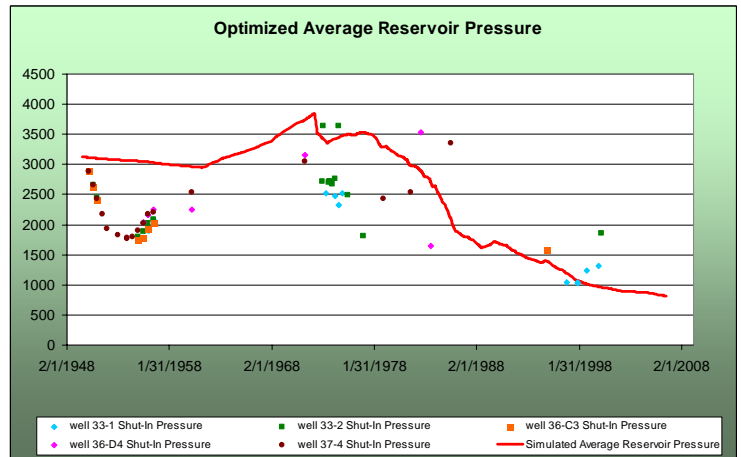


Figure 38: History Match of Average Reservoir Pressure

Note: actual pressure measurements were originally Shut-in pressures. Peaceman's correction was applied to those pressures to be properly compared to Average Reservoir pressure.

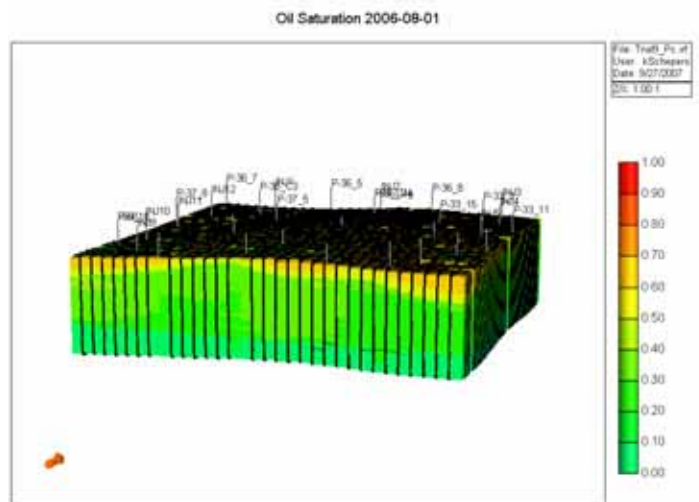


Figure 39: 3D View of Residual Oil Saturation at the End of the Simulation